Diamond-Like Carbon Coatings for Tribology: Production Techniques, Characterization Methods and Applications

S.V. Hainsworth & N.J. Uhure

Department of Engineering, University of Leicester, University Road, Leicester, LE1 7RH

Abstract

There are numerous types of surface coatings available to engineers in order to improve the friction and wear resistance of components. In order to successfully use these coatings in practice, it is important to understand the different types of coatings available, and the factors that control their mechanical and tribological properties. This paper will focus on the application of diamond-like carbon (DLC) coatings in tribological applications. Thus far, DLC coatings have found broad industrial application, particularly in optical and electronic areas. In tribological applications, DLC coatings are now being used successfully as coatings for ball bearings where they decrease the friction coefficient between the ball and race, in shaving applications where they increase the life of razor blades in wet shaving applications, and increasingly in automotive applications such as racing engines and standard production vehicles. The structure and mechanical properties of DLC coatings are dependent on the deposition method and the incorporation of additional elements such as nitrogen, hydrogen, silicon and metal dopants. These additional elements control the hardness of the resultant film, the level of residual stress and the tribological properties. As diamond-like carbon films increasingly become adopted for use in industry, it is important to review the factors that control their

properties, and thus, the ultimate performance of these coated components in practical tribological applications.

Introduction

DLC is a generic term that is commonly used to describe a range of different types of amorphous carbon films. These films include hydrogen-free diamond-like carbon, a-C, hydrogenated DLC, a-C:H, tetrahedral amorphous carbon, ta-C, hydrogenated tetrahedral amorphous carbon, ta-C:H, and those containing dopants of either silicon or metal such as Si-DLC and Me-DLC respectively. This terminology is discussed in more detail in the next section. In order to differentiate between the types of DLC being referred to, we have used the specific film type rather than the generic term as far as possible. "Diamond-like" as a term reflects the fact that films contain some proportion of sp^3 bonding, in reality the mechanical properties of the resultant films can be very different to the properties of diamond.

DLC coatings are increasingly being used to improve the tribological performance of engineering components. The coatings can possess high hardness, low coefficients of friction against materials such as steel, and they are generally chemically inert. These desirable tribological properties arise as the properties of the film can be manipulated to give either diamond-like or graphite-like properties by controlling the deposition process. Additionally, the incorporation of nitrogen, hydrogen, silicon or metal-doping gives further possibilities of controlling the chemistry, and thus the tribochemistry of the films.

In addition to the excellent mechanical properties, DLC coatings can be smooth, pinhole and defect free and provide a good diffusion barrier to moisture and gases.[1]

In the past, two factors have limited the further exploitation of DLC, the first of these is that the coating thickness is limited by the build up of residual stress as film thicknesses increase which can lead to delamination failure and the second factor is that at relatively low temperatures (250˚C) the properties begin to degrade as DLC converts to graphite. By 400˚C this graphitisation process is rapid. This generally limits the maximum service temperature of DLC to around 250-300˚C.

The thermal properties of DLC can be manipulated by the deposition process. The thermal conductivity of DLC can vary between 400-1000$Wm^{-1}K^{-1}$ depending on deposition conditions which has lead to its exploitation as a heat spreader in microelectronic applications[2] but the good conduction of heat is also desirable in tribological applications where the temperature of sliding contact is important as it can help prevent hot spots during sliding. Other factors such as the ambient temperature are also important in determining the nature of the friction and wear observed for DLC films.

DLC films initially found application in improving the tribology of magnetic-head sliders and magnetic storage media.[3] For these applications, the contact stresses and operating temperatures are relatively low and therefore DLC performs well.

In recent years, there has been more emphasis on applying DLC films to mass-produced mechanical components, particularly in the automotive sector. The films are used to reduce frictional losses in higher stress contact and reliability and coating cost are important to their success.

This paper will review the various types of diamond-like carbon coatings that can be produced and in particular those that have been applied in tribological applications, their structure, the different deposition methods available, methods for evaluating their mechanical and tribological

properties and the factors that are important in influencing their tribological response. Not all potential processes become industrially robust and successful.

A selected range of properties for the various diamond-like carbon films, along with the properties of diamond and graphite, are presented in Table 1.[4-25] Additional information on properties can also be found in VDI guideline 2840.[11]

Types of diamond-like coatings

Terminology

There are several types of diamond-like carbon films which depend on the proportion of sp^2/sp^3-bonded carbon, and additional elements such as silicon, hydrogen and metal/carbide dopants. It is therefore important to identify the terminology that will be used in this paper. The abbreviation DLC in itself can be misleading as often the properties vary considerably from diamond but the term in this paper will be used as a general term to classify films in the generic family of amorphous carbon coatings. A hydrogen-free amorphous carbon film with prevailing sp^2-bonding will be denoted a-C, a hydrogenated film with a similar modest sp^3 fraction termed a-C:H. Films containing hydrogen with a more substantial proportion of sp^3 bonding will be denoted ta-C:H (where ta denotes tetrahedral amorphous). Films with a significant fraction of sp^3-bonded carbon (>70%) will be denoted by ta-C. Those films doped with silicon or metal/carbide dopants will be denoted Si-DLC and Me-DLC respectively.

Bonding of Carbon.

The mechanical and tribological properties of the family of diamond and diamond-like carbon films is largely controlled by the sp^2/sp^3 ratio. In the ground state of carbon, the electrons exist as $2s^2$, $2px^1$, $2py^1$ which means that stable σ bonds can form with two other atoms. It is also possible to promote one the of the s electrons into the 2pz orbital to obtain a structure of $2s^1$, $2px^1$, $2py^1$, $2pz^1$. The energy required for this promotion is small since it reduces the electronic repulsion between electrons in the 2s orbital. Also, the promotion is energetically favourable owing to the stronger bonds that can be formed. The $2s^1$, $2px^1$, $2py^1$, $2pz^1$ gives 4 unpaired electrons that can allow σ bonds to be formed with four other atoms by a process of forming sp^3

hybrid orbitals which arrange in a tetragonal configuration. sp^2 hybrid orbitals can also be formed where the electron in the s orbital hybridizes with 2 of the p orbitals to give 3 orbitals with a 120˚ in plane bond angle. One of the p-orbitals is left unaffected and overlaps with those from neighboring carbon atoms, in a sideways manner, to form the distributed out of plane π-bonds that reside above and below the in-plane bonds. The 3 different bonding configurations are shown in figure 1.[26] If the carbon is bonded in the sp^2 configuration this forms the graphite structure which has strong bonds within the plane, but weaker, van der Waals bonds between the planes. As an example, the bonding energy for the σ bonds is ~7.4eV whereas the bonding energy for the van der Waals bonds between the graphite planes is only ~0.86eV.[27] The graphite structure therefore has mechanical properties that are strongly directional, and graphite can easily be sheared between the layers. This means that graphite can be used as a solid lubricant. The sp^3-bonded carbon leads to a tetrahedral arrangement of bonds and the diamond structure. This gives a 3 dimensional network of bonds and materials with good isotropic mechanical properties. The carbon-carbon bond lengths are short with high bonding energies and the diamond structure thus has stiff bonds and a high elastic modulus and hardness.

The 3D structures of graphite and diamond resulting from the differing hybridisations are shown schematically in figure 2.

Diamond-like carbon films are composed of small crystallites that have a local configuration, which is either sp^2 or sp^3. Thus DLC has a random stable network but the size of the clusters is sufficiently small that electron diffraction techniques reveal an amorphous material and DLC has no long range order.[28]

Deposition methods – Advantages and Disadvantages of the Different Techniques.

Diamond-Like Carbon Films

There are numerous deposition methods that can be used to deposit DLC films. Recent reviews in this area can be found by Lifshitz[27] and Wei and Narayan.[29] Generally, the films are produced either by PVD or by CVD methods. In contrast to the production of diamond films, DLC films can be deposited at room temperatures. The resultant films are structurally amorphous. Figure 3 shows a schematic ternary phase diagram[26] for the different carbon films that can be formed as a function of the sp^2 or sp^3 bonding fraction and the amount of H contained within the films. The differing deposition processes that can be used for the production of DLC films have differing electron or ion energies, differing precursor gases or target materials and differing temperatures and therefore films can be produced with a vast array of properties from the soft and lubricating a:C-H through to ta-C films with properties close to that of diamond.

The deposition techniques can be separated into plasma vapour deposition (PVD) and chemical vapour deposition (CVD). A brief description of the most common techniques for depositing DLC films is given below.

PVD processes

There are many different variants of the PVD process. All involve condensation of a vapour in a high vacuum (typically 10^{-6}-10^{-8} Pa) atomistically onto a substrate surface. PVD processes are line of sight so complex geometries and holes may cause difficulties in obtaining a uniform coating. PVD processes include evaporation, sputtering and ion plating (or ion beam assisted deposition).

Sputtering

Sputtering offers a highly controllable method for depositing DLC films and is the most common industrial process for the deposition of DLC films. In sputtering, an inert gas (typically argon) is ionized by electrons emitted from a cathode (for DLC, graphite cathodes are used). The Ar^+ ions accelerate to the cathode where they sputter away the cathode material. The main sputtering processes for DLC are dc diode sputtering or rf sputtering. Graphite sputters relatively slowly and thus additional techniques are used to improve coating deposition rates. The most common of these techniques is unbalanced magnetron sputtering (figure 4). In this process, magnets are placed behind the graphite cathode(s). The magnetic field causes the electrons ejected from the cathode to spiral and increase their path length, which gives a higher degree of plasma ionization. The magnetic field is "unbalanced" by arranging the magnets so that the magnetic field passes across the substrate and thus the Ar ions bombard the substrate as well as the target material. This ion bombardment promotes sp^3 bonding in the coating and gives denser films and higher deposition rates. Reactive magnetron sputtering is widely used in industry[31-33] to prepare coatings such as W-DLC. In this process, transition metal targets are used along with a reactive gas, usually acetylene to form the resultant compound coatings, with the transition metal being incorporated into the film in the form of carbides.

Ion beam deposition

Ion beam sputtering or deposition (IBD) uses a beam of Ar ions to sputter carbon from a graphite target. A schematic of this deposition method is shown in figure 5. An advantage of this technique is that high quality coatings can be deposited at low temperatures (near room temperature). However, the deposition rate is low (max. 1μm/hour) and the films can often be low density as the atoms have low mobility during the deposition process. In addition, the

substrates have to be manipulated to ensure uniform deposition. The ion beam process can be improved in several ways, either heating the substrate or allowing ion bombardment of the coating as it grows. Heating of the substrate can lead to distortion or softening which is undesirable so ion plating or ion beam assisted deposition (IBAD) are often preferred. In ion plating, a small negative charge is applied to the components to be coated and a proportion of the coating flux is ionized by either passing the flux through a plasma, or by using a hot filament to generate a flux of electrons into the system or by using an arc evaporation process. In IBAD, a second Ar ion beam is used to bombard the film that helps to densify the coating and/or encourage sp^3 bonding. The ion bombardment processes can lead to heating of the substrate material so the processes need to be carefully controlled. IBAD is a commercial scale deposition technique.

Cathodic Arc

Cathodic arc is a complex technique for producing DLC films, but has the advantage that the resultant films have excellent mechanical properties. This technique is also used for producing commercial coatings. For DLC films, a graphite cathode is struck by a carbon striker electrode in a high vacuum (typically 10^{-5} to 10^{-3} Torr) and then withdrawn in order to initiate an arc discharge. This can take place in a reactive or non-reactive environment, and results in an energetic plasma with a very high ion density ($<10^{13}$ cm^3). The power supply required to maintain the arc discharge is a low voltage, high current supply (on the order of 15 to 150 V and 20 to 200 A, respectively).[5] The arc spot formed on the cathode is of a small diameter (1 to 10 μm), and carries an extremely high current density (10^6 to 10^8 A cm^{-2})[26] which not only produces the plasma, but also releases micrometer-sized particulates from the cathode which can result in rough surfaces, in turn leading to film failure due to cracks initiated at grain boundaries. The

formation of these droplets is an unwanted by-product of the explosive emission process that removes the evaporant species from the cathode surface, and to counteract this the plasma can be passed through a magnetic filter, a method known as filtered cathodic vacuum arc (FCVA) (figure 6).

In FCVA an electrostatic field is produced owing to the plasma electrons spiralling around the magnetic field lines, which in turn attracts the positively charged ions to follow the same path around the filter. Since the droplets cannot follow the field, they are deposited on the walls of the filter. Sanders and Pyle[36] reported that controlling the plasma in this way resulted in the deposition rate increasing by a factor of 4, and adhesion to the substrate increasing by a factor of 6. Introducing baffles along the filter and/or by constructing an 'S' shaped filter can improve the filtering capabilities by a factor of 100.[37-42] Another advantage of FCVA is that, unlike IBD, the depositing plasma beam is neutral, and hence can deposit films onto insulating surfaces. The disadvantages of this method are the relative complexity, insufficient filtering ability for certain applications (e.g. super smooth films required for optical coatings) and a potentially unstable cathode spot. Cathode spot instability, however, can be reduced by re-striking the arc or by using a magnetic field at the cathode to steer the spot around the cathode surface.[43, 44]. Pulsed-arc deposition where pulsing is achieved by either filtered laser-induced vacuum arc or filtered high current pulsed arc has been used to produce ta-C films with high hardnesses and low friction.[45] These films can be produced on insulating substrates at modest temperatures and are nearly particle free.

Gupta and Bhushan[46] investigated the tribological and mechanical properties of a-C films as deposited by cathodic arc, ion beam deposition, radio frequency-plasma-enhanced chemical vapour deposition (r.f.-PECVD) and r.f. sputtering techniques. It was found that films deposited

by cathodic arc possessed the highest hardness (38 GPa), Young's Modulus (350 GPa), scratch resistance/adhesion and residual compressive stress (12.5 GPa). Anders *et al*[47] reported an even higher hardness of cathodic arc a-C films of 45 GPa measured by nanoindentation, this was attributed to the high percentage (>50%) of sp^3-bonded carbon.

Pulsed Laser Deposition

A review of amorphous diamond-like carbon films produced by pulsed laser deposition is given by Voevodin and Donley.[48] Pulsed laser deposition is a versatile laboratory scale method for the deposition of many different materials. In PLD for carbon coatings, a pulsed excimer laser beam of short pulse and high energy is directed onto a pure graphite target (99.9%) in a vacuum chamber evacuated to between 10^{-3} and 10^{-6} Pa (see figure 7). This produces a plasma plume of evaporated/ablated material that condenses onto the cold substrate. The resultant mechanical properties of the films are dependent on the properties of the plume, which is in turn influenced by the fluence and wavelength of the laser, the substrate temperature and the hydrogen content. Ta-C films with sp^3 contents of between 70 to 95% can be produced by this method.

CVD Processes

Chemical vapour deposition methods are high temperature thermo-chemical processes where substrate temperatures are usually required to be maintained in the range 800-1000ºC. In CVD processes, a chemical reaction occurs above the substrate where the chemicals decompose and then recombine to form the required coating on the heated substrate. The elevated substrate temperatures limits the components that can be coated to materials not affected by the high temperatures (e.g. sintered carbide), or necessitates post-coat heat treatment to restore the original properties of heat-sensitive substrate materials. CVD processes produce uniform coatings with high hardness and good adhesion to the substrate (assuming the coating is not too

thick). However, coatings are limited to ~10μm due to differential thermal expansion mismatch stresses, and there are environmental concerns with regards to the process gases. Processes such as PECVD have been developed to allow CVD coatings to be deposited at lower substrate temperatures.

PECVD

Plasma-enhanced or plasma assisted chemical vapour deposition, PECVD or PACVD, is a hybrid process whereby the chemical vapour deposition (CVD) processes are activated by energetic electrons (100 to 300eV) within the plasma as opposed to thermal energy in conventional CVD techniques. PECVD is a vacuum-based deposition process operating at pressures ranging from 0.01 to 5 Torr, (typically <0.1 Torr),[5] allowing the deposition of DLC films at relatively low substrate temperatures ranging from 100°C to 600°C (typically <300°C). Whereas the plasmas created in PVD processes such as sputtering are initiated by inert precursor gases with high ionisation potentials (e.g. argon), PECVD tends to use gases that are more easily ionisable. Initially benzene was used as the precursor gas but this requires high bias voltages for the process. Acetylene is the more usually preferred choice now for mechanical applications but is less popular for coatings for electronic applications since it is not available in a high purity form and therefore methane is the gas of choice for optoelectronic applications.

Plasmas can be generated by dc, high-frequency radio frequency (typically 13.56 MHz) or microwave (typically 2.45 GHz) fields. A popular configuration used for rf-PECVD deposition incorporates a reactor with two electrodes of differing area.[26] The smaller substrate electrode is coupled capacitively with the rf power and the larger electrode is earthed. This produces a positively-charged plasma with an excess of ions, whilst both electrodes acquire a dc self-bias potential that is negative with respect to the plasma. The substrate electrode is of a smaller size

and therefore has a smaller capacitance than the larger electrode. It acquires a larger self-bias voltage thereby becoming negative relative to the larger electrode, and subsequently subject to ion bombardment from the plasma. Increasing the rf power has been found to increase the sp^3-bonded carbon in DLC films,[49] and films deposited at a bias voltage below 200 V possess an extremely low coefficient of friction below 0.05.[50]

Since PECVD requires relatively low substrate temperatures and high deposition rates are attainable, films can be deposited onto large-area substrates that cannot withstand the high temperatures required for traditional CVD techniques (typically >600°C). This permits the deposition of films onto steel surfaces, which would otherwise experience detrimental effects to mechanical properties, and even onto polymers that would be completely unstable at such elevated temperatures. Unlike CVD, PECVD also allows thick coatings (>10μm) to be deposited onto a substrate with a differing thermal expansion coefficient without having stresses develop during the cooling period. It has been found that DLC films deposited by pulsed PECVD have lower internal stresses, leading to improved adhesion on steel substrates.[51]

PECVD has been found to be successful in combination with PVD deposition where the PVD process is used to deposit interlayers of titanium and silicon followed by PACVD of the a-C:H layer.[52, 53] Coatings produced by this route are widely used in a number of industrial applications such as plastics injection moulding tools and racing engine applications.

Techniques for Characterizing the Properties of DLC coatings

There are a number of techniques that are commonly used for evaluating the tribological performance and mechanical properties of diamond-like carbon coatings. Tests for mechanical property assessment include hardness and nanoindentation testing and wear testing. Adhesion

and fracture toughness of the coatings have been assessed by a number of methods and these are briefly reviewed below.

Hardness and Nanoindentation Testing

Hardness testing has long been used for evaluation the near-surface mechanical properties of materials and is ideal for measuring the properties of coatings. Microindentation testing is of some benefit as it is cheap, simple to perform and widely available but it is difficult to separate out the relative contributions of the film and substrate to the measured hardness. Additionally, for DLC films, cracking is common and may appear as nested cracks around the indentation periphery as seen in figure 8. This can make it difficult to identify the indentation size and thus lead to uncertainty in the calculated hardness values.

More recently, nanoindentation has become a widely used technique for measuring the elastic modulus and hardness of coatings. In nanoindentation tests, the force and displacement of an indenter into a sample are recorded as a function of time to produce a mechanical fingerprint of the materials response to the indentation.[54] The advantage of nanoindentation over conventional hardness testing is that indentations can be made at smaller loads as the residual impression does not need to be measured optically. This allows indentations to be made to a small fraction of the coating thickness, and thus the mechanical properties of the coating can be measured in relative isolation of the substrate material. The rule of thumb is that for the measured hardness to be that of the coating alone the indentation depth should be confined to approximately one tenth of the coating thickness, this is supported by experimental and theoretical results. This rule does not hold for the modulus, as the elastic foundation for the coating (i.e. the substrate) can influence the measured modulus at ratios considerably less than $1/100^{th}$ of the coating thickness.[55-57] The hardness and modulus are usually calculated from the unloading curve of the nanoindentation

load-displacement response using the analysis of Oliver and Pharr[58] which was developed from an earlier approach to this taken by Doerner and Nix.[59] The method of Oliver and Pharr has been further developed by Pharr *et al*[60] to account for the geometrical shape of the indenter. In order to obtain the materials elastic modulus, the analysis method consists of fitting the unloading curve of the nanoindentation response with a power law relationship. The elastic modulus is found from a modified form of Sneddons relationship,[61] vis:

$$S = \frac{dP}{dh} = 2\beta\sqrt{\pi}\, E_r A_r$$

where S is the unloading stiffness, β is a constant (1.034), E_r is the reduced elastic modulus A_r is the area of contact.

The contact area is obtained from $A=f(h_c)$ where h_c is the contact depth. This contact depth can also be used for obtaining the hardness which is simply the force divided by the area. One important difference between hardness measured using nanoindentation techniques and a traditional microindentation tester is that the area measured using nanoindentation uses projected area whilst the hardness measured using a Vickers indenter is measured using surface area and thus care must be taken in converting data between the two types of test. (Projected area is preferable as it relates more closely to the yield stress for most materials).[62, 63] The area function for the indenter is determined experimentally from indentations into materials with known elastic moduli and accounts for the fact that the indenter is not perfectly sharp at shallow indentation depths. It is important that the nanoindenter is accurately calibrated before performing indentations and procedures for this can be found in the relevant ISO standard.[64] The surface roughness of the material to be tested should also ideally be known.

Various studies of DLC coatings have been performed using nanoindentation testing.[65-75] The substrate contribution to the measured response is important. For example, a C:H deposited onto relatively soft stainless steel shows cracking at relatively low loads caused as the brittle coating bends and flexes into the substrate.[76] In cases where the coating is deposited onto harder substrates such as tool steel[66] the differing regions of the underlying microsctructure can be differentiated in the measured nanoindentation response. Even at low loads (1mN) the substrate influences the measured response, not only because of the differing substrate mechanical properties but also because of the differing residual stress states and microstructures of the resultant coatings. Changes in the mechanical response are further complicated by the fact that often the coatings possess differing numbers, thicknesses and types of interlayers used to promote adhesion.

As an example of a nanoindentation into a DLC coating, figure 9 shows a typical load-displacement curve for a 10mN nanoindentation into a PACVD DLC coating on a hardened steel substrate. The coating is a multilayer coating comprising of a 1μm thick titanium nitride layer followed by a 1μm thick silicon layer deposited by PVD with a final 1μm layer of a-C:H deposited by PACVD. The coating contains approximately 10% atomic hydrogen.[52, 77] Figures 10a and 10b show SEM micrographs of two higher load (500 and 250mN) indentations. It can be seen that at 500mN there is pronounced cracking within the indentation but this cracking has disappeared at 250mN where it is difficult to distinguish the indentation other than in the plastic creases where the coating has conformed and bent to the indenter geometry. These indentations illustrate the benefits of nanoindentation where the hardness can be calculated from the load-displacement curve rather than needing to try and measure the indentation diameters as in microhardness testing.

In order to attempt to separate effects from film and substrate, various models have been developed to analyse indentation and nanoindentation data. The aim of these models is to determine the relative contributions of the film and substrate to the measured or composite hardness. One of the earliest models in this area was developed by Jönsson and Hogmark[78] whose model was based on the relative area fractions of film and substrate supporting the load. Burnett and Rickerby[79] proposed an alternative approach based on the relative volumes of film and substrate that support the load. The Jönsson and Hogmark model works on the assumption of large penetrations and cracking of the film. The Burnett and Rickerby model works well for cases where plasticity dominates, i.e. there is no fracture, or where the indenter penetration is low and cracking is not well established. When cracking dominates, the fit of data to the model is less satisfactory.

An improved model for fitting indentation sizes across the range of indentation load or size where both plasticity and cracking are in turn dominant was developed by Korsunsky *et al*.[80] This model uses a fit to the composite hardness data against the relative indentation depth, β., i.e. δ/t where δ is the indentation depth and t is the coating thickness. The fit is of the form

$$H_c = H_s + \frac{H_f - H_S}{1 + k\beta^2}$$

where H_c is the composite hardness, $H_{s,}$ the substrate hardness, H_f the film hardness, and k a constant obtained from the fitting procedure. The model was developed to fit data obtained across the nanoindentation, microindentation, macroindentation range. This model can be successfully applied to obtain hardness values of the film in isolation of the substrate. An example of the fit for a PACVD a-C:H coating is shown in figure 11. The fit gives a film

hardness of 25.7GPa. The calculated film modulus was found to be ~200GPa and was constant with penetration depth.

Adhesion Testing

The adhesion of a film to the substrate on which it has been deposited is integral to the overall tribological performance of the coating. It is a compound property dependent on the substrate, coating and the deposition method. A recent review of adhesion testing by Volinsky *et al*[81] indicates that there are over 200 methods for assessing adhesion. Several of the most practical and widely available are briefly reviewed here.

From an industrial standpoint, one of the most widely used tests for coating acceptance is the Mercedes Benz or Rockwell C indentation test. The Rockwell-C indentation test is a quick and easy to perform destructive test that can be used as a quality control tool for the manufacture of coated materials. The method was developed in Germany and the guidelines are set out in the VDI 3198 guideline.[82]

The test uses a conical indenter to penetrate into the surface of a coating, causing extensive plastic deformation of the substrate and fracture of the coating. The total depth of indentation should be less than one tenth of the specimen thickness. During indentation the interface experiences extreme shear stresses, and whereas a strongly adhered coating will withstand these stresses, films with poor adhesive qualities will exhibit delamination around the indentation imprint.

The adhesion is qualified by the test as either sufficient or insufficient. These qualifications are assessed by examining the cracking pattern around the indentation as shown in figure 12. HF1 – HF4 represent acceptable failure modes whilst HF5 and HF6 represent unacceptable failure

modes. The results from a Rockwell C adhesion test can also be used to give a qualitative indication of the fracture toughness as a brittle film will have a number of radial micro-cracks in the vicinity of the indentation.

One other common way of assessing coating adhesion is the scratch test. In this test, a stylus (usually a diamond cone) is drawn over the coating surface with an increasing normal load. The minimum critical load (L_C) at which delamination occurs gives a measure of the practical work of adhesion. Sometimes the subscripts L_{c1}, L_{c2}, L_{c3} etc. are used to define different failure modes in the same scratch. Scratch testing requires care in the interpretation of results as not all failures result in a delamination of the coating from the substrate and therefore it may not always be possible to quantify the adhesion. The scratch test failure mode can also vary widely for different coating substrate combinations and therefore direct comparison of results between different film substrate combinations can be difficult. The different failure modes that are observed in scratch testing are described in detail by e.g. Bull.[83] Despite the difficulties and limitations associated with interpreting the failures, scratch testing is widely used. The failure modes that are observed depend not only on the type of DLC coating but also on the load support from the substrate. For example, figure 13a shows forward chevron cracking in a PACVD a-C:H coating on a nitrided steel substrate whereas figure 13b shows the same coating simply on a steel substrate and shows a wedge spallation failure mode.

Wear testing of DLC coatings

DLC is often used to improve the wear resistance and durability of components. In order to accurately determine the performance of the coatings, robust wear testing techniques are required. A number of wear tests have been successfully used to assess the wear of coatings such as pin on disk, reciprocating sliding wear and the dry sand rubber wheel test.[84-87] However,

there can be difficulties in using these tests on thin hard coatings where in order to accurately assess the wear rate of the coating only small amounts of wear can be tolerated. This in turn causes difficulty in assessing the wear volume as measuring the mass loss is fraught with difficulties and profilometry is prone to errors as the depth of wear damage is of the order of uncertainty of measurement from the original surface finish of the sample. Other techniques that are commonly used for assessing wear resistance include multi-pass scratch testing[88, 89] and microabrasion (or ball-cratering) wear testing.[90-98]

Microabrasion wear testing (or ball cratering) is a popular technique for assessing the abrasive wear resistance of thin hard coatings. In this test, a ball is rotated against a sample under a known load with an abrasive suspension or slurry of (usually) fine (2-10μm) SiC (or Al_2O_3) particles in water. There are three common variants of the test, a rotating wheel (dimpler) type instrument developed from dimpler grinders used for TEM specimen preparation, a free ball system where the rotation of the ball is driven by friction and a fixed ball system where the ball is driven directly by clamping the ball in a split drive shaft. All of these result in a spherical depression in the sample. The diameter of the impression can be used to calculate the wear volume of the material. Tests can be performed for different durations, the coating usually perforates relatively quickly, and the wear coefficients for both the coating and substrate can be extracted from the results. For reproducible results it is important that the condition of the ball surface, load, speed, temperature, humidity and slurry feed are carefully controlled to ensure that three-body rolling abrasion conditions are satisfied.[92, 93, 96, 98]

Micro-abrasion testing of DLC coatings can be difficult depending on the exact nature of the DLC. Flaking can occur around the crater edges.[99] Also, the wear damage is often uneven with some regions showing extensive wear and pitting and other regions appearing smooth and

undamaged. This has been attributed to variations in structure arising from clusters of sp^2 or sp^3 hybridisations within an amorphous DLC matrix. Harder sp^3-bonded DLC regions are expected to be more wear resistant than softer sp^2 regions.[100] However, the concept of ball cratering does give a route to testing the abrasive wear resistance of extremely thin (t ~100nm) DLC films such as those for MEMS applications.[101] An example of a good microabrasion wear test is shown in figure 14. This reveals an a-C:H topcoat, SiC interlayer and a TiN adhesion promoting layer. The central region is the steel substrate. As can be seen from the micrograph a further advantage of microabrasion wear testing is that the layer thickness can be calculated from the SEM micrograph and thus microabrasion wear testing is often used as a quality control tool for film thickness determination.

The adhesive wear of DLC coatings is often assessed by pin-on-disk wear testing or reciprocating wear testing (see ASTM G99[102] and ASTM G133[103] respectively). In order to give reliable results, laboratory scale wear tests should be conducted with experimental conditions (load, speed, contact geometry, temperature) as close as possible to those seen by the component in service. If this is the case, there is usually good confidence that the tests will select the best wear-resistant coating. However, it can be difficult to mimic in-service conditions and in these cases there is often a large discrepancy between the laboratory prediction and the in-service performance.

Fracture Toughness

Nastasi *et al*[104] used microindentation to investigate the fracture toughness of DLC coatings on Si substrates. The presence of the DLC coating reduced the size of radial cracks produced as compared the crack length in uncoated silicon. The effective fracture toughness was calculated from

$$K_r = \chi \frac{P}{C^{3/2}}$$

where P is the applied indenter load, C is the half-crack length and x is a material constant.[105] For brittle materials, χ is taken as $0.016(E/H)^{1/2}$, where H is the projected hardness and E is the Young's modulus. This approach assumes that the stress intensity factor for DLC coated silicon is the same as that for silicon and that the cracks are in the form of half-penny (radial) cracks. This indentation approach to measuring fracture toughness for DLC yields values of toughness of the order of 10.1MPa $m^{1/2}$ which is much higher than that predicted from bond breaking calculations (which gives 1.5 MPa $m^{1/2}$)[105] and approximately twice that of the uncoated Si substrate. The differences are attributed to either plastic work and/or complicated path cracks and/or deviations from the half-penny crack geometry in the DLC coating/Si substrate system. In order to obtain the fracture toughness of the DLC alone, the relative contributions to the toughness of the coating and substrate are deconvoluted by comparing the relative proportions of the crack surface area in the coating and the substrate.

An alternative method for obtaining the fracture toughness of DLC coatings was used by Li *et al*.[75] They found that cracking occurred in 3 stages, initially ring-like through thickness cracks formed through the coating thickness followed by delamination and buckling and finally secondary ring cracks and spallation (see figure 15). The fracture toughness is then calculated from the strain energy release in cracking which is estimated from a step in the loading portion of the load-displacement curve. The values of fracture toughness obtained ranged between 4.9 to 10.9 MPa $m^{1/2}$.

Indentation-based approaches to measuring fracture toughness make assumptions about the crack geometry in coated systems being similar to those in bulk materials. The presence of the coating

may modify the size and shape of cracks and therefore it is likely that the real fracture surface areas differ from those where the crack geometry is well controlled. These differences will affect the estimation of the total elastic work in the models, and therefore the values obtained must be viewed with caution.

Measurement of sp^2/sp^3 ratio

The properties of diamond and DLC films depend on the type of bonding that is present, the hydrogen and nitrogen content, and in particular the sp^2/sp^3 ratio. The bonding of the films can be determined using a number of techniques including NMR, ESCA, EELS, XPS, visible and UV Raman, spectroscopic ellipsometry and diffraction based techniques including electron, X-ray and neutron diffraction.[26] Of these techniques, the two that are most commonly used (currently) for characterizing the bonding types are EELS[106] and visible Raman although UV Raman is becoming an increasingly important technique.

EELS is the most common technique for determining the sp^3 fraction in DLC films. In EELS, the transmission electron microscope is used to pass an electron beam through a thin film. The film is typically 10-20nm thick to avoid problems from multiple scattering and the film is debonded from the substrate material so the technique is destructive. The transmitted beam is inelastically scattered by the sample and the energy change is detected on a spectrometer. The results are plotted as intensity in arbitrary units against energy in eV and a typical trace for various carbons is shown in figure 16. For sp^2 bonding in graphite, a peak occurs at 285eV. For diamond sp^3 bonding, a step is observed at 290eV. The sp^2 fraction of a film can be determined by taking a ratio of the area under the graphite and diamond peaks respectively for a given energy window (say 284 to 310eV).[106, 107] This can be compared to the ratio observed for a

100% sp^2 sample of randomly oriented micro-crystalline graphite. More details on this technique can be found in e.g.[26]

Visible Raman has also been widely used for determining the bonding types in DLC because it has the advantage of being non-destructive and the analysis can usually be performed with the film in situ on the substrate. Also, the film thickness is not critical. In visible Raman (using either 488 or 514.5nm lines from an Ar^+ ion laser corresponding to energies of 2.55 and 2.42eV) photons are used to irradiate a sample and a proportion of the scattered radiation from the sample shows shifts in frequencies that are characteristic of the vibrational transitions occurring in the sample (the Raman effect). A typical Raman spectra from different carbons is shown in figure 17. There are two peaks that are commonly seen, and these are denoted D and G for disorder and graphite and occur at 1332cm^{-1} and 1550cm^{-1}, respectively. Visible Raman only has sufficient energy to excite sp^2 vibrations, the higher energy of UV Raman at 244nm (5.1eV) is required to excite vibrations from sp^3-bonded carbon. Nevertheless, visible Raman can be used to determine the sp^2/sp^3 fraction which has usually been extracted from shift or broadening of the peak that occurs at 1550cm^{-1}.[108] The accuracy of determining the sp^2/sp^3 ratio is relatively low, ±10%, but it does give the information quickly and non-destructively compared to the other techniques.

UV Raman is gaining in popularity for investigating DLC because the energy (5.1eV) is sufficient to excite sp^3 vibrations. The UV Raman spectrum can be correlated with the sp^3 fraction by studying the position of an additional peak that is observed in UV Raman, the T peak. The T peak arises from sp^3-bonded atoms and is observed at a Raman shift of 1050cm^{-1}. The intensities of the T and G peaks are obtained to give an I(T)/I(G) ratio which is found to increase in a systematic fashion with increasing sp^3 ratio.[109-111] NMR can also be used to quantify the

sp^2/sp^3 ratio, the most direct method being C^{13} NMR.[112-121] The separate graphitic and tetrahedral configurations each produce a chemically-shifted peak, determined by molecular standards.

Residual Stress and Techniques for Residual Stress Measurement

Typical DLC films have high levels of residual stress (up to 10GPa). The level of residual stress plays an important part in determining the mechanical properties and adhesion of DLC films. Because DLC is amorphous, measurement of residual stress cannot be performed by diffraction-based techniques such as X-ray diffraction, which use the crystal structure as an atomic strain gauge. The main techniques that have been used for measuring residual stress in DLC films are beam curvature and Raman.

The basic concept of beam curvature methods is that the curvature induced by coating a thin strip of substrate is dependent on the residual stress in the film. There are various methods for measuring the curvature of the beam, and commonly laser reflection is used. The Stoney equation[122] is then used to determine the residual stress, σ_r

$$\sigma_r = \kappa \bar{E}_s h_s^2 / 6h$$

where κ is the curvature of the film/substrate system, $\bar{E}_s$ is the biaxial Young's modulus of the substrate and h and h_s are the thickness of the film and substrate respectively.

Raman spectroscopy can also be used for measuring residual stress. Stresses within the coating lead to a change in the equilibrium separation between the constituent atoms. This changes the interatomic force constants that determine the atomic vibrational frequencies. A compressive stress leads to a decrease in bond length and an increase in vibrational frequency (or vice versa for tensile stresses). The result of this is to cause a shift in the peak position observed in laser

Raman spectroscopy, in particular, the G peak. The amount of the shift can be correlated against a stress free reference sample. The magnitude of the shift is related to the residual stress by the equation

$$\sigma = 2G[(1+\upsilon)/(1-\upsilon)](\Delta\omega/\omega_0)$$

where $\Delta\omega$ is the shift in the Raman wavenumber, ω_0 is a reference wavenumber, G is the shear modulus and ν the Poisson's ratio of the material respectively. If a stress free reference sample is unavailable then the peak shift for a given stress can be determined by beam bending[123] which allows comparison of the stress level with a known applied stress.

Factors Affecting the Mechanical and Tribological Performance of DLC Coatings

Hydrogenated DLC Films (a-C:H)

The doping of a-C and ta-C DLC films with hydrogen and its effect on the structure and tribological performance has been the subject of extensive investigation.[9, 124-126] The inclusion of hydrogen is believed to pacify dangling bonds in the DLC structure, in turn reducing the defect coordination density and promoting the tetrahedral bonding of the carbon atoms. Therefore, a highly hydrogenated film possesses a high sp^3 content. The downside of a-C:H coatings is a reduction in cross-linking, leading to a lower density (approximately 1800kgm^{-3} less than graphite and diamond), and a lower hardness as the film becomes more polymeric in nature, despite the increased sp^3 content.

The relative hydrogen content of a DLC film can be determined by a number of techniques including proton nuclear magnetic resonance (NMR), nuclear reaction analysis (NRA), combustion analysis and secondary ion mass spectroscopy (SIMS). Fourier Transform Infra-Red

spectroscopy (FTIR) and elastic recoil detection (ERD) are used to quantify the hydrocarbons groups present. Despite the number of available approaches, the exact proportion of carbon-bonded hydrogen is difficult to quantify and measures of relative hydrogen content are the best available.[5]

Hydrogen plays a critical role in the tribology of DLC films. The friction of diamond, diamond-like and graphite-like DLC films is highly dependent on both the test environment and the gaseous species such as hydrogen that are incorporated into their structure.[127-131] Films that contain little or no hydrogen in their bulk or surface structure or films that are tested in a hydrogen free environment often give very high coefficients of friction[125, 127, 129, 131, 132] whereas films derived from highly hydrogenated discharge plasmas can have extremely low friction coefficients (of the order of ~0.01 or below).[125, 132, 133] This indicates that the termination states of the surface are important in determining the tribological behaviour. Thus, if the surfaces are terminated by e.g. hydrogen or oxygen and thus relatively inert, their coefficients of friction tend to be low. However, if the surfaces are not well terminated and thus chemically active (i.e. some of their covalent σ-bonds are available for bonding) the friction coefficients of the films may be very high. This has been attributed to the possibility of strong covalent bond interactions across the sliding interfaces. Other chemical and physical interactions can occur such as van der Waals forces, electrostatic attractions, weak $\pi-\pi^*$ attractions (particularly for graphitic films) and capillary forces and contribute to the overall friction that is observed.[132]

The wear rate is also affected by the hydrogen content. Jones *et al*[134] studied the tribology of hydrogen free and conventional hydrogenated DLC films. The films in their study were produced by close field unbalanced magnetron sputter ion plating. They found that hydrogen free films showed improved wear resistance in pin-on-disc and reciprocating wear tests. This

may be linked to the higher hardness values of the hydrogen free films giving improved abrasive wear resistance.

Nitrogenated DLC Films (a-C:H:N)

Nitrogen-doped DLC films (a-C:H:N) have been investigated in order to determine how various levels of N_2 introduced at the deposition stage effect certain properties of the film. Whereas hydrogen is believed to stabilize the sp^3 bonding states, the addition of N_2 to the hydrocarbon precursors increases the sp^2/sp^3 ratio by encouraging C sp^2 bonding. This modification of chemical bonding within the DLC structure can be analysed via Raman spectroscopy, where an increased N content is accompanied by a broadening of the D band, as C atoms in aromatic sp^2 clusters are substituted by N atoms and hence produce an increased lattice disorder.

Nitrogen also has a significant effect on the tribological properties of DLC films. Lin *et al*,[135] conducted a detailed study of the effect of N on mechanical properties. They produced a range of films on silicon with nitrogen contents of 0, 25, 40 and 66 vol %. For 0 and 25 vol. % nitrogen, the hardness increased with film thickness from 50 to 300 nm. For 40 and 66 vol % nitrogen, the effects of film thickness were less clear, and for 66%, chipping around the indentations was observed. The N_2-free film possessed the highest Young's Modulus. The decrease in surface hardness of a-C:H:N over N_2-free films has been linked possibly to increased lattice disorder, or the formation of C=N bonds reducing the interlinks of sp^2 clusters.[135]

Guerino *et al*[136] also observed that increasing the proportion of N_2 in a $CH_4/Ar/N_2$ plasma during reactive sputtering substantially increased the deposition rate. The sputtering rate of films is usually expected to decrease by some degree when doping is undertaken, due to the lower sputtering yields of chemically different compounds when compared to the original surface elements. However, with N_2-doped a-C:H films the opposite occurs, and the deposition rate was

seen to increase by approximately 50%. This was attributed either to the reaction of reactive N_2 atoms with the target C atoms and with the C_xH_x ions[137] in the plasma and substrate surface, or that plasmas containing N_2 are denser than N_2-free plasmas. The correlation between nitrogen content, film thickness and film hardness for a given deposition time of 15 minutes is presented in Figure 18**.**

The inclusion of N_2 in a-C:H films is thus a double-edged sword: the film thickness is increased from the enhanced sputtering rate but the N_2 doping affects chemical bonding leading to a decreased hardness over equivalent N_2-free films.

Si-DLC Films

Si-DLC films generally have excellent tribological properties such as very low friction, good durability, good stability in humid environments and improved high temperature performance.[138-141]

The effect of silicon on the structure of Si-DLC films has been investigated using transmission electron microscopy (TEM), Fourier Transform Infra-red spectroscopy (FTIR),[20] X-ray Absorption Near Edge Structure (XANES) and Extended X-ray Absorption Fine Structure Spectroscopy (EXAFS).[142] These studies showed Si-DLC films to have an amorphous structure. Si suppresses the formation of aromatic structures and promotes the diamond-like character of the films by forming tetrahedral bonds with hydrogen and CH_n groups.[20] The films have short range order where each Si atom is co-ordinated to four carbon atoms or CH_n groups.[142]

In terms of the resultant properties, incorporating silicon into the DLC structure improves adhesion to the substrate[143] and the strength of the films.[23, 144] It has also been shown to reduce the compressive stress[21, 145] which has the advantage that thicker films can be produced. Si-

containing DLCs up to 10μm in thickness can be produced in contrast to DLCs with no silicon which are typically 1-4μm thick. The addition of silicon has also been shown to improve the thermal stability of the films. Si-free DLC films generally start to oxidise and degrade after exposure to temperatures in the region of 300˚C.[8] Above 300˚C hydrogen is liberated and the films convert to graphite.[146] Si-DLC films deposited on Si and subsequently annealed in argon environments at temperatures of 670˚C for one hour showed little visible change and a small amount of graphitization in Raman spectra[145] whereas baking Si-free DLC in vacuum causes flaking at 400˚C and complete delamination of the film at temperatures of 550˚C.[147] However, a 200˚C anneal in argon has been shown to decrease the residual compressive stress and reduce the cohesion and adhesion failure loads of Si-DLC deposited on AISI 4340 low alloy and AISI 440 C high alloy steel specimens.[148]

One of the main reasons for incorporating silicon into DLC is that it has been found to reduce the dynamic friction coefficient in ambient humidities (>2%RH)[140, 145, 149, 150] where the tribological properties of conventional Si-free DLC deteriorate.[130, 131] The associated wear rate of Si-DLC films is generally higher, sometimes only slightly,[145, 151] but increases of as much as a factor of 4 have been seen.[149] The reduction in friction coefficient has been attributed to both the formation of SiO_2 at the frictional interface,[140, 141] and an increase in the sp^3 content to give a less graphitic film.[145] Si has also been shown to increase the coefficient of friction of the films when used in dry atmospheres[149] so it is important that the exact chemistry of the film is tailored to give the optimum friction and wear performance for a given set of operating conditions. The static coefficient of friction of DLC is not heavily influenced by Si incorporation.[152] The SiO_2 formation will account for the increased wear as this thin soft surface layer is readily removed by sliding.[153]

Si-DLC coatings have been tested with a range of oils. For example, Ban *et al*[154] studied the performance of Si-DLC using ball-on-disk tests with an oil containing zinc dialkyldithiophosphate (Zn-DTP) additives and compared this tests using an oil without the additive. The films were immersed in oil and tests were conducted at 80˚C using a smooth bearing steel ball as the counterface. Si-DLC films showed low coefficients of friction and low wear in tests with the additive containing oil. X-ray photoelectron spectroscopy (XPS) showed that a boundary lubrication layer formed in the lubricated contact region to separate the surfaces and keep the friction coefficient and wear rate low.

Me-DLC films and other alloying additions

Metal-doping or carbide-doping has been developed to try and improve DLC films by enhancing adhesion, thermal stability and toughness. These films can be considered to be nanocomposite structures and have been shown to offer improved hardness and elastic modulus or to give a combination of hardness and ductility. PVD-prepared carbide-doped hydrogenated DLCs are commercially available, one in particular being tungsten carbide-doped (WC/C) DLC, a chemically inert film with high elasticity and good wear resistance. The hardness is tailored by the coating process and can range from 500 to 2500VHN.[155] During deposition, the carbide phase is grown by direct current (DC) magnetron sputtering and the carbon phase is grown simultaneously from a hydrocarbon and argon plasma, in which the hydrocarbons contain a mix of acetylene and C_2H_2.

Most mechanical property measurements on Me-DLC films have been conducted on W-DLC films.[14-17] For these films, the Young's modulus ranges from 100-120GPa. W-DLC films are typically in residual compression with a residual stress of ~ 900MPa.[15] Fracture toughness measurements conducted on W-DLC films determined the toughness (depending on the yield

response of the steel substrate) to be 30-35 Jm^{-2} (~ 1.8-2.0MPa$\sqrt{m}$) from the critical strain for channel cracking.[15]

A Cr-adhesion layer with a W-DLC coating on a steel substrate showed an interface toughness superior to that of DLC alone.[15] The advantage of this is that failure occurs within the DLC itself rather than at the coating-substrate interface.

The incorporation of fluorine in DLC films has been investigated[156-160] and found to increase the hydrophobicity of DLC as it has the effect of lowering the surface energy of the resultant film, although films with a high fluorine content suffer by way of increased mechanical instability, resulting in reduced hardness and modulus.

Influence of the substrate

The overall coating thickness of DLC films is commonly between 1-4μm or even thinner. This means that the substrate plays a considerable role in supporting the applied load in any application. If the substrate is not sufficiently hard, and stiff, then either flexure of the substrate material, or plastic deformation and yielding in the substrate will lead to premature coating failure. A range of strategies has therefore been employed to ensure that the substrate is sufficiently hard and rigid. For example, Podgornik & Vizintin[161] used a duplex treatment where AISI 4140 steel was plasma nitrided prior to coating deposition. Plasma nitriding to case depths of 0.3 or 0.55 mm was found to improve both the wear resistance and effective adhesion (for the adhesion tests used) of a ta-C coating over a hardening treatment alone.

Film Roughness

The tribological properties and overall effectiveness of a DLC film when used as a solid lubricant is strongly influenced by the surface roughness of the film.[162]

The roughness of DLC films has been shown to depend on the various deposition methods[163, 164] and deposition parameters such as ion energy,[165-170] gas mixture[163] and bias voltage.[169]

Coating roughness is also dependent on substrate material[171-173] and the underlying substrate roughness. Increasing the substrate temperature during deposition results in a higher proportion of sp^2 bonding, creating a more graphitic and therefore rougher surface.[165, 174, 175] Conversely, at temperatures between 700°C and 900°C, film smoothing occurred as an increase in surface diffusion rate accompanied the presence of atomic hydrogen.[176]

The effect that film thickness has on film roughness has also been studied.[177, 178] For thin CVD films (<200nm) deposited at 90° to the substrate, the growth of the films obeys the ballistic model[179] whereby initially, growth on the asperities occurs at a higher rate than within the troughs, causing the film to be rougher than the substrate surface. This then gives way to a gradual reduction in roughness with each successive DLC layer, as the troughs in the previous layer are filled.

The coating roughness can be modified by a number of methods such as Ar ion bombardment, hydrogen etching and heat treatment after deposition in order to produce optimum properties.

Interlayers

DLC films possess a high level of intrinsic residual stress and this is a direct contribution to their poor adhesion to steel substrates. This lack of adhesion restricts the thickness, and the incompatibility between the DLC/steel interface can result in delamination at low loads. To combat these problems, interlayers of various metallic and ceramic compounds have been incorporated into the design of coated systems, which have been shown to relax the compressive stress of DLC films, increasing adhesion and the load-carrying capabilities. An example of a

multi-layer a-C:H coating is shown in figure 19. This shows (from bottom upwards) a steel substrate, TiN layer for promoting adhesion, a SiC layer followed by a final a-C:H topcoat. Each layer is approximately 1μm in thickness.

Chen *et al*[180] investigated chromium interlayers as a method improving the adhesion of DLC on stainless steel (SKD11). The films were deposited by inductively coupled plasma (ICP) CVD, the Cr interlayers by magnetron sputtering with substrate bias. Chromium is an attractive candidate for an interlayer material in conjunction with a steel substrate, due to the similar thermal expansion coefficients (11.8 x 10^{-6} and 12.5 x 10^{-6} °C, respectively) and high toughness ensuring low thermal stress and high bonding strength. Results showed that in this configuration, intermediate adhesion of HF3 was attained with Rockwell adhesion testing. However with further intermixing of the Cr-steel interface from ion bombardment, adhesion was greatly increased to HF1.

The tribological properties of a thick DLC coating with a graded and multi-layered structure were investigated by Xiang *et al*.[181] Cr layers were again found to improve adhesion, whilst the transitional section that comprised CrN_z and C_xCr_y layers increased the load bearing capacity. The film possessed a Vickers hardness of 1560 VHN at 250g, favourable adhesive qualities (with a scratch test critical load, L_c at 52N) without catastrophic failure and a low friction coefficient of 0.09.

Chang and Wang[143] investigated the tribological performance of DLC films with various Ti-based interfaces deposited onto M2 steel substrates. The results in figure 20 show the increase in adhesive strength at L_c = 20N for a-C:H to L_c = 70N for DLC with a Ti/TiN/TiCN transition layer.

Silicon-based interlayers have similarly been found to promote the adhesive qualities between DLC films and various substrates.[182, 183]

Ageing of DLC/Temperature Dependence of Properties

DLC films often possess poor thermomechanical stability, as the films are susceptible to hydrogen loss and rapid wear and graphitisation at elevated temperatures.[86, 184] Doped films (Si-DLC, Ti-DLC, a-C:H:N) show improved durability at high temperatures due to retardation of the graphitisation process.

Incorporation of Si into DLC films prepared by PECVD processes has been shown to reduce the intense ion bombardment that occurs in the PECVD process and thus reduce the intrinsic stress in the films which allows thicker films to be deposited.[185, 186] The Si also has additional benefits in that it acts to promote the production of sp^3-bonded C.[187] Coatings produced by this method have been shown to have improved hardness values after nanoindentation testing of films previously annealed at temperatures up to 400°,[188] with no spontaneous delamination observed. Higher temperatures resulted in structural changes, decreasing the hardness and fracture toughness of the films.

Bull and Hainsworth[189] showed that the nanoindentation response of rf-PECVD and IBAD DLC films changed over a period of 5 years when stored at room temperature (see figure 21). Both films exhibited a gradual reduction in the elastic properties, as well as their hardness to a lesser extent. The decrease in modulus (42% for rf-PECVD; 58% for IBAD) accompanied a relaxation of the compressive residual stress produced during deposition, and a reduction in density as C–C and C–H bonds break and reform over time.

Effect of Operating Environment

The environment significantly affects the tribological properties of a DLC film, a situation further complicated by the complex relationships between the various deposition parameters, the atmospheric conditions and the lubricious and mechanical and chemical properties of the coating and the nature of the counterface. Often, the friction and wear of the contacting surfaces are controlled by the formation of transfer layers (or tribolayers).

Highly hydrogenated a-C:H film in inert gas environments exhibit an extremely low friction coefficient (~0.003), whereas a ta-C film with zero H content has a very high coefficient (~0.71) under the same conditions. In order for a non-hydrogenated a-C film to possess a low friction coefficient, moisture at the sliding surface is required.[125] It was also found that in open air, the friction coefficient of a-C film dropped by 62% whilst a highly hydrogenated a-C:H film's coefficient rose by 200%.

Relative humidity (RH) also plays a major part in determining the tribological properties of unlubricated DLC films. Kim *et al*[128] showed that in a wear test of a PECVD film against a Si_3N_4 ball, the lowest wear rates were in dry environments (of the order of 10^{-9} $mm^3N^{-1}m^{-1}$ for 0% RH air and 0% RH argon). In dry argon, adhesive wear was the dominant wear mechanism, with the lowest friction coefficient (0.06), low wear rate of the DLC film and undetectable wear of the ball attributed to a film of wear debris transferred from the DLC, completely covering the ball. In 0% RH air, a dry oxidised transfer layer of DLC covered the ball, causing the low wear rate and an intermediate friction coefficient of 0.16. At the other end of the scale in 100% RH air, the same species of wear debris was observed as with dry air, but in this case it was concluded that the additional water molecules in the humid environment caused strong adhesion of the wear debris to the DLC film, hence resulting in a high friction coefficient of 0.16. In

humid argon, the oxidation of the DLC filmed occurred at a much slower rate as the oxygen required for this reaction is only provided by water molecules absorbed by the wear debris, resulting in a decrease in friction coefficient (0.2 to 0.09) over 60 minutes as the layer of wear debris formed on the ball. In a similar investigation conducted by Ozmen *et al*,[190] a layer of transferred wear debris was also observed and deemed responsible for a high friction coefficient in 80% RH. Additionally, the increase in the failure load in high humidity conditions was thought due to the water molecules saturating on the film surface, reducing the number of dangling bonds between film and counterface and hence preventing bond formation. Singer et al[191] using a tribometer with in-siut Raman, found that a transfer layer of graphite-like carbon was important in controlling the friction of DLC contacts.

The effect of water lubrication has been investigated by Ronkainen *et al*.[192] a-C and ta-C films showed excellent wear resistance ($<10^{-}9 mm^3N^{-1}m^{-1}$) and initially high friction coefficients that decreased with time (approx. 0.6 to 0.05 and 0.2 to 0.04, respectively). This was due to the high roughness and high hardness of the as-deposited films being smoothed over time. A single-layered a-C:H coating suffered severe wear during the test and could not survive in water-lubricated conditions. It was found that using multilayers or doping (especially with Si) improved greatly the friction and wear performance of hydrogenated amorphous carbon coatings.

In this age of environmental consciousness, water-based lubricants have been investigated as a viable alternative to traditional lubricating oils, which in conjunction with DLC-coated materials can meet the demands of the present industry requirements. Persson and Gahlin[193] found that the friction coefficient during a pin-on-disc wear test was determined by the lubricant (in the case of good lubricants), but more importantly it was reduced by the DLC film for poor lubricants. The

DLC coatings were also responsible for increasing the resistance to seizure, with a much more noticeable effect with water-based lubricants than with pure oil or distilled water.

The introduction of DLC coating in automotive applications to meet the increasing demand for greater performance, fuel economy and wear life of engine and transmission components has necessitated studies into the tribological behaviour of the films under oil-lubricated conditions. By their very nature, DLC coatings possess a very low surface energy, and this "inertness" has in the past raised the question whether or not there is true boundary lubrication between DLC/DLC contacts. Engine and transmission development has been accompanied by the advanced chemical development of oil additives, with anti-wear (AW) and extreme-pressure (EP) additives considered critical in reducing wear and friction between surfaces under severe boundary-lubrication conditions.[194, 195] The tribochemical reaction between uncoated metallic surfaces and the molecules of the additives result in the formation of tribofilms, the chemical composition of which determining it's lubricious efficiency. It is widely accepted that the formation of phosphates results in reduced wear, whereas the presence of sulfides reduces the friction.[196-198] The complex interactions between the many coating types, contact combinations (DLC/DLC, DLC/steel etc.), dopants, oil types and additives, as well as the influence of operating parameters such as the oil temperature, contact geometries and load, indicates that this particular area will require extensive future research to provide optimum combinations for different applications.

In studies of various coating combinations and oils with differing chemical compositions,[19, 199] tests conducted under severe boundary-lubrication conditions showed that wear of uncoated steel/steel contacts was lower than for steel/DLC and DLC/DLC, regardless of oil type. The inclusion of additives greatly reduces the wear rate for both DLC/DLC contacts (up to 80% for the tungsten-doped DLC & up to 60% for a-C:H), indicating that the inert coatings *do* provide

boundary lubrication. Increasing the EP additive concentration has been shown to reduce friction and wear of W-DLC/steel contacts, whilst having no discernible affect on pure DLC coatings.[200]

Natural biodegradable oils containing high amounts of unsaturated molecular bonds and polar groups have been shown to improve the tribological performance significantly where one or more surfaces is DLC-coated. Lubrication by non-polar mineral oil resulted in higher friction coefficients and poor wear as well as different wear mechanisms.[199]

Practical applications of DLC

DLC coatings have been successfully employed in a number of tribological applications. The most common (or well-known) application of DLC is to razor blades such as the Gillette DLC™ and the Wilkinson Sword FX Diamond™, as shown in figure 22. Manufacturers advertising claims improved performance over traditional stainless steel blades. Many of the industrially important applications of DLC can be found in the patent literature. Current more technological explotiation of DLC coatings is in applications such as bearings, pistons for motors and pumps and driving elements such as gears and shafts.[201] DLC coatings are widely used in the automotive industry. A typical range of parts that can benefit from DLC coating are shown in figures 23 and 24. It was estimated that nearly 30 million coated parts were supplied to the automotive industry annually in 2001 and that this figure would rise by 50% annually.[202] DLC coatings on tappets have been shown to give a 1% improvement in fuel economy and a reduction in CO_2 emissions.[203] Arps *et al*[204] have used ion beam assisted deposition of DLC to coat critical components in a diesel engine such as the rocker shaft and roller pin. The DLC coatings in their study were bonded with an intermediate layer of silicon that reacts to form a metal silicide and promotes adhesion. Pin-on-flat wear testing was performed under conditions of load,

temperature and lubrication analogous to that in an engine and the coatings were found to give a significant reduction in wear-rate over bare metal, or DLC without the bond-coat. Me-C:H coatings have been used to improve the performance of gears, bearings, piston rings and the cam-tappet contact.[202] Currently one of the largest industrial applications of DLC coatings is for diesel fuel injection systems. The injection pressures in these systems has risen over recent years to meet ever stringent emissions targets. The increase in pressure has meant that components like pump plungers are often coated with DLC so that the surface can withstand the higher requirements for adhesive wear resistance.[202] The Organisation Internationale Des Constructeurs D'automobiles expects global production of automobiles to be 70 million in 2006 and of which diesel vehicles account for ~23% of the market.

In addition to the choice of DLC, two other factors are important in automotive applications, whether to use DLC surfaces in contact with DLC, and the choice of lubricant. Recently, Podgornik *et al*,[205] showed that a DLC/steel combination gave a smoother running-in process as compared to DLC/DLC or steel/steel combinations. They used extreme-pressure and anti-wear additives at low sliding speeds and a range of loads to ensure boundary lubrication conditions. The tribological performance of tungsten carbide-doped DLC coatings with water-based lubricants has also been investigated.[193] The results of these tests showed that the lubricant does not always reduce the coefficient of friction, however, it is possible to get results similar to those obtained with oils for certain "good" lubricants although the exact chemistry of "good" lubricants is not considered.

DLC has found good application in biomedical areas where its biocompatibility and corrosion resistance allows it to be used in tribological applications such as coatings for hip joints and knee replacements. For these applications the coatings need to be high quality with excellent adhesion

to the substrate, good surface finish and good corrosion resistance.[53, 206] A recent review of diamond-like films for medical prostheses discusses the use of DLC on biosensors and cardiovascular devices in greater detail.[207]

DLC coatings have achieved considerable success over the last decade, future competition may arise as superlattice coatings and hybrid nanocomposite coatings emerge from the research field and onto the market.[208] Fullerene-like CNx coatings are currently being tested in practical applications and are good candidate low friction and low wear materials.[209] However, given the considerable impetus that diamond-like carbon films have achieved they are likely to remain practical solutions to many engineering problems for a long-time to come.

Conclusions

This paper has reviewed the production techniques, characterization methods and applications of diamond-like carbon coatings. Diamond-like carbon coatings possess very attractive tribological properties that can be tailored by altering the sp^2/sp^3 ratio and by understanding the environment in which the coating will operate. DLC coatings are available in a number of different forms which give differing levels of hardness and modulus, residual stress and dopant atoms which control their mechanical and tribological properties. Each type of coating has different advantages and the entire range of properties should be studied carefully to select the optimum coating for a given application.

Amorphous carbon films are typically 1-5μm thick. Hydrogen-free amorphous carbon coatings (a-C) are generally rich in sp^2-bonded carbon and therefore relatively soft. In dry atmospheres a-C films have higher coefficients of friction than hydrogenated amorphous carbon a-C:H films. a-C:H coatings, which have a range of hardnesses depending on their hydrogen content (lower

hydrogen contents giving harder films), give low friction coefficients in dry atmospheres up to high loads but can give high wear on the counterpart because of their high hardness. Additionally, as the humidity increases the friction coefficient can rise considerably. Similar problems can occur with ta-C coatings that contain high fractions of sp^3-bonded carbon and thus high hardness and subsequent high counterface wear. Si-doped DLCs and ion beam deposited coatings are stable and give very low friction coefficients in dry sliding conditions, with Si-DLC also providing a lower friction coefficient in higher relative humidity. Me-C:H coatings have been successful in a number of automotive applications. The metallic elements are incorporated into the films in the form of carbides and modify (improve) coating adhesion and tribological properties.

DLC coatings have found application in a diverse number of fields from medical to automotive and they will increasingly find application in other areas as the demands on materials to perform at higher contact loads and operating speeds is increased to meet environmental challenges in emissions for example. One of the main challenges to users of DLC coatings is in selecting the correct type of film for a given application but improved data on the response of different coatings under standard tests should ultimately provide the information necessary to underpin successful design involving DLC coatings.

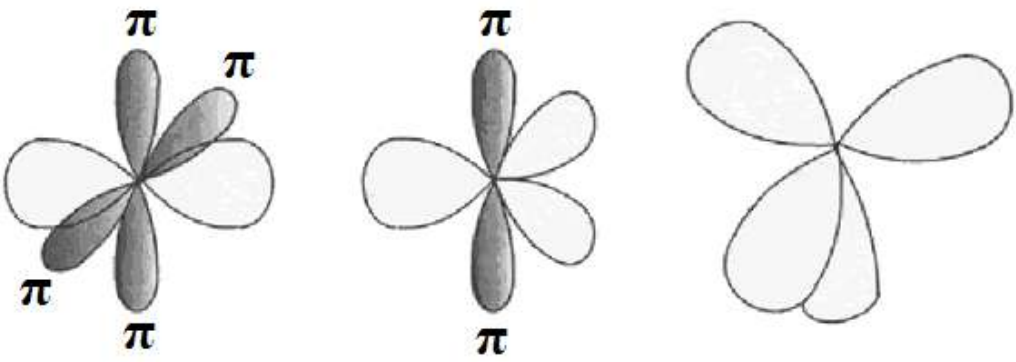

a) sp^1 b) sp^2 c) sp^3

Figure 1: Schematic of the different possible bonding states for C atoms.[26] a) sp^1 hybridisation with two available in-plane σ bonds in x and π bonds in y and z. b) the three-fold directed sp^2 hybrids oriented for in-plane σ bonding with a weak π orbitals for out of plane bonding c) tetrahedral sp^3 hybrids that form σ bonds with adjacent atoms

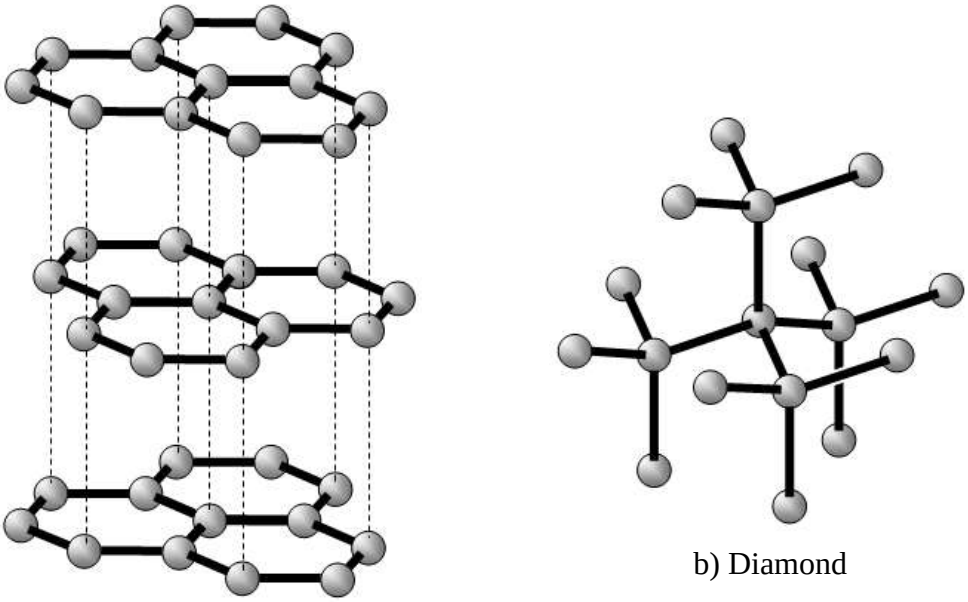

a) Graphite b) Diamond

Figure 2: The graphite and diamond structures that result from the differing hybridisations of carbon atoms.

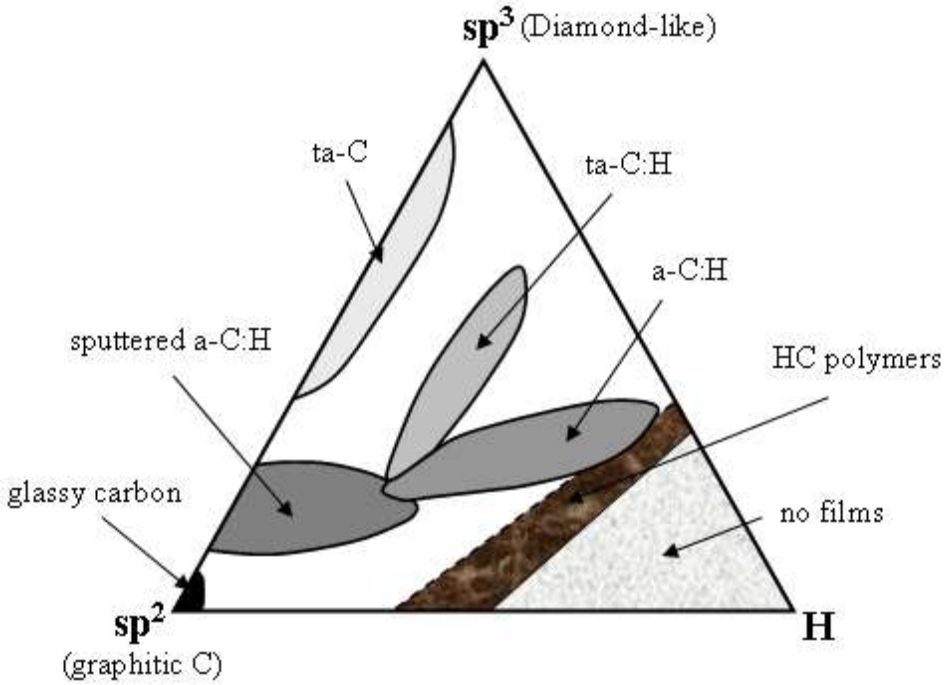

Figure 3: Ternary phase diagram showing the different possibilities for forming the different carbon films as a function of C bonding and H content[26]

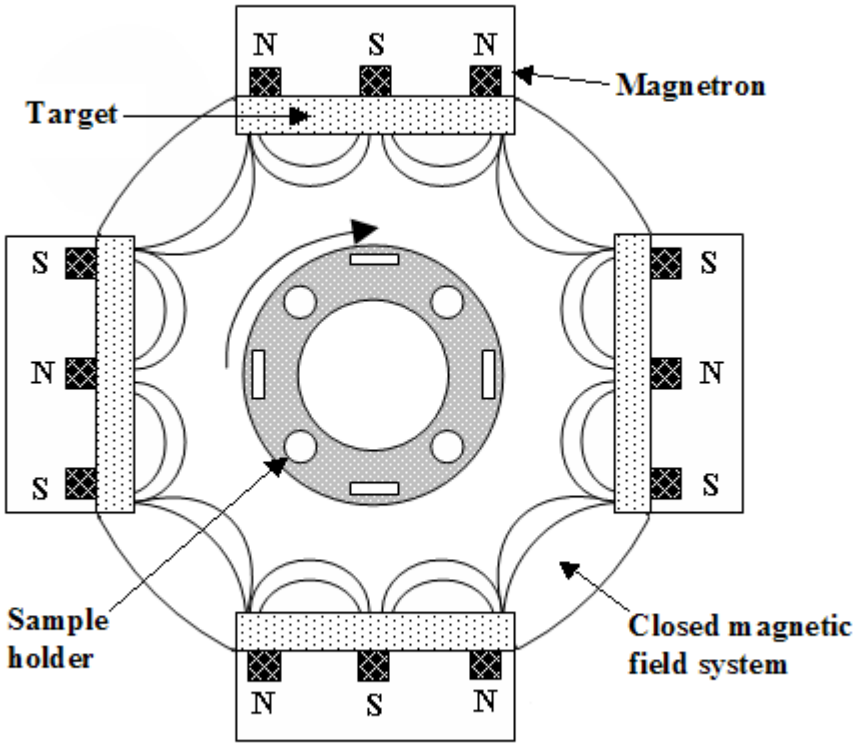

Figure 4: Schematic of a closed field unbalanced magnetron sputtering ion plating system[30]

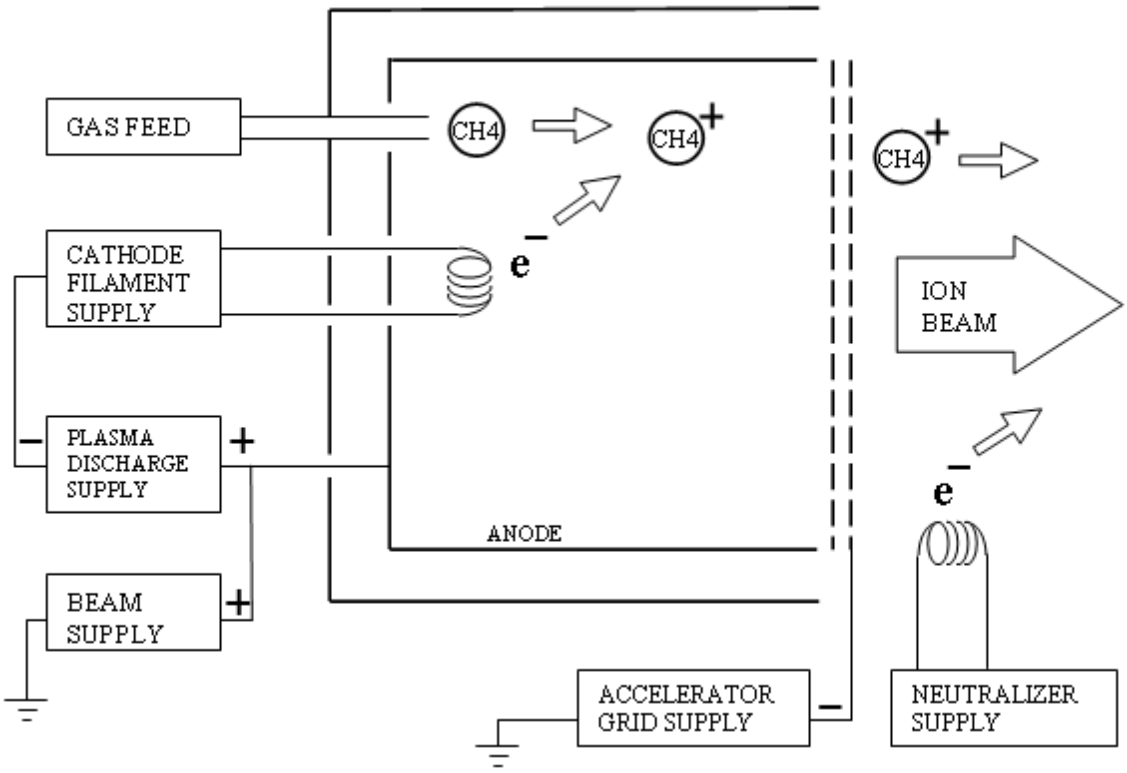

Figure 5: Schematic of an ion beam deposition system[31]

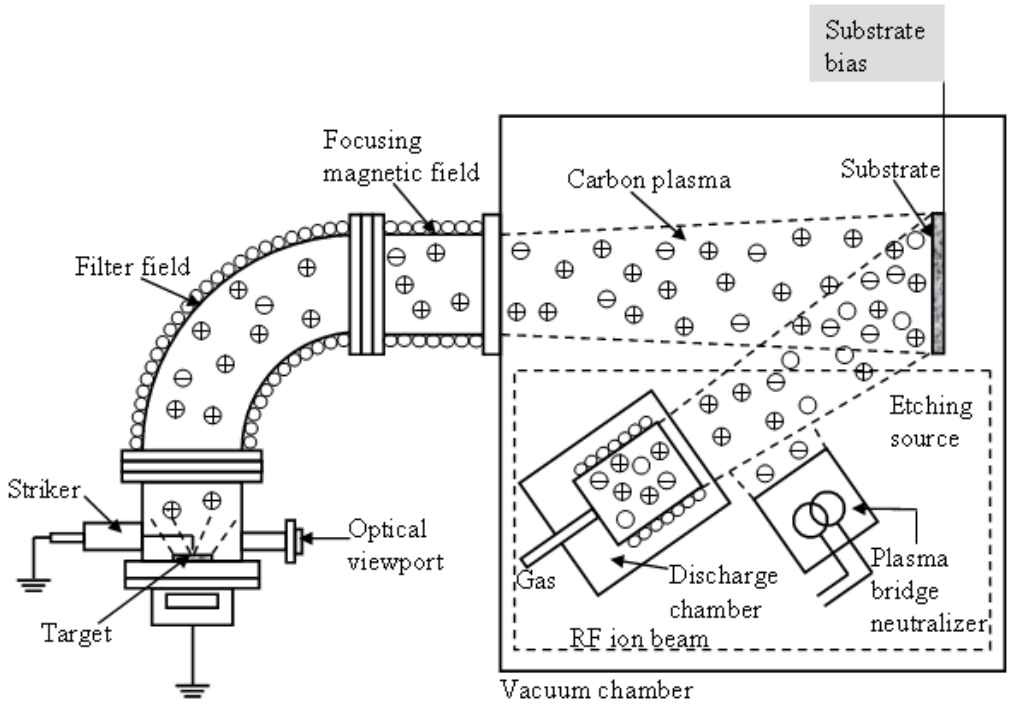

Figure 6: Schematic of a filtered cathodic vacuum arc deposition system (FCVA)[32]

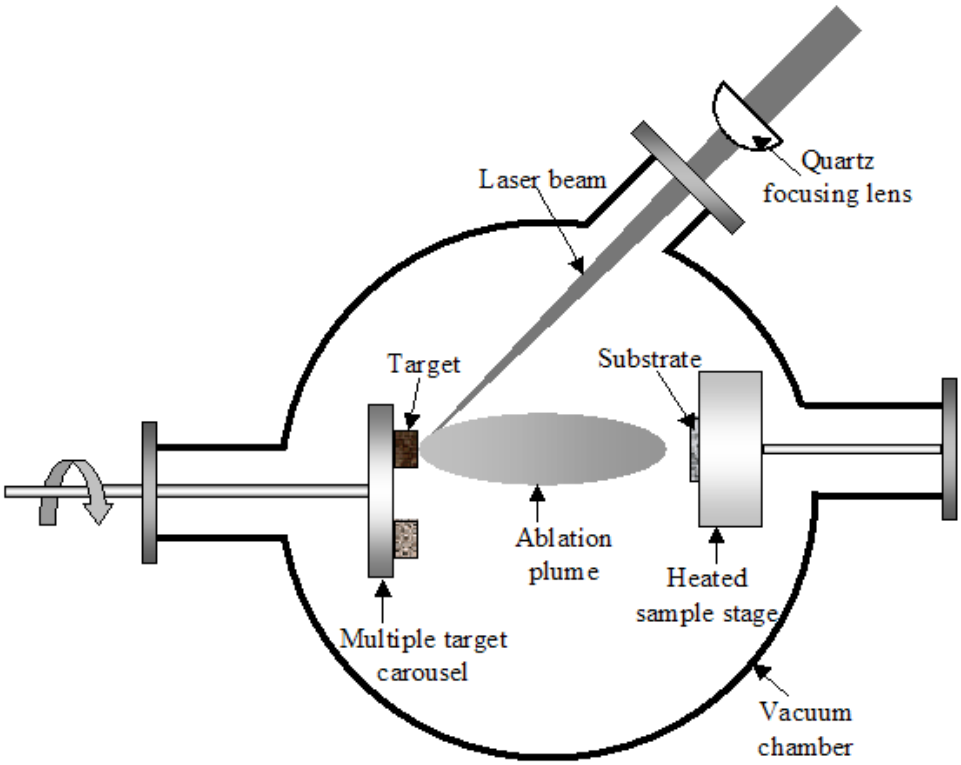

Figure 7: Schematic of a pulsed laser deposition system[44]

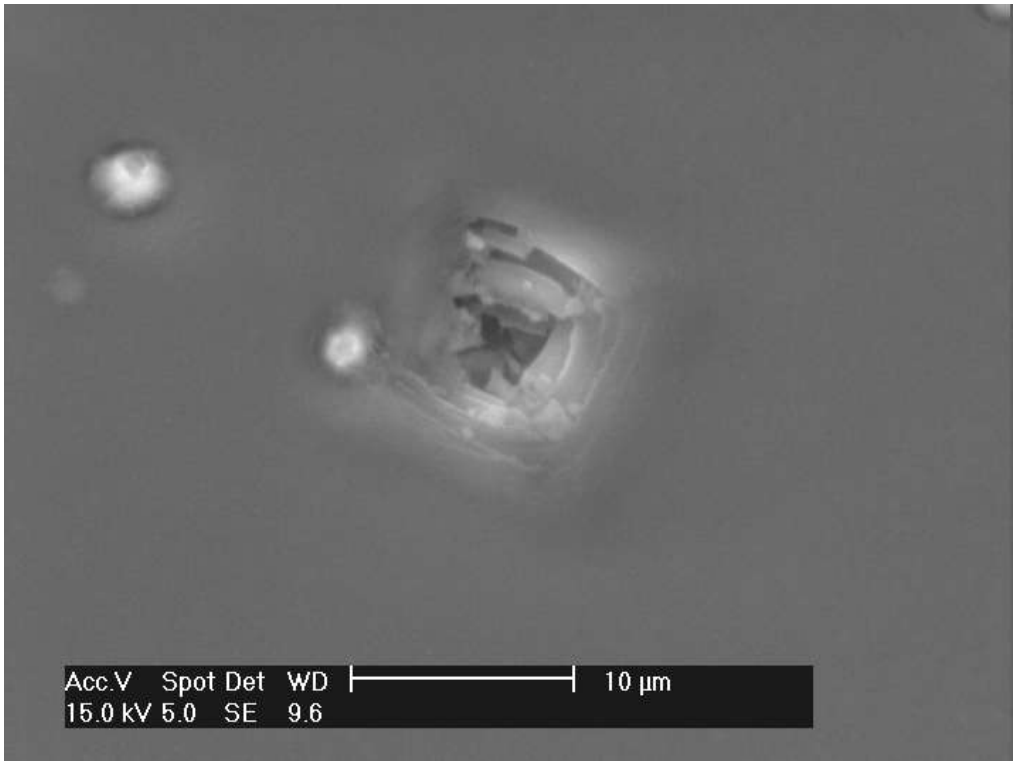

Figure 8: Nested cracks around a 200gf microindentation on a DLC film. The cracking makes it difficult to accurately identify the corners of the indentation and leads to uncertainty in the calculated microhardness values.

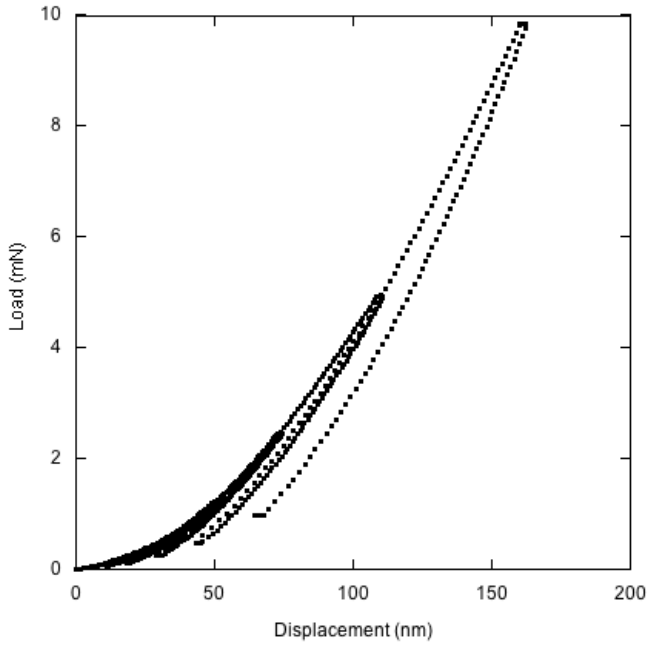

Figure 9: Typical nanoindentation load-displacement curve for a 10mN indentation in a PACVD a-C:H coating. The graph shows five load-unload cycles at different proportions of the maximum load (10mN) which show that the coating loads in a repeatable manner with no viscoelastic deformation. The hardness and modulus can be calculated from each load-unload cycle.

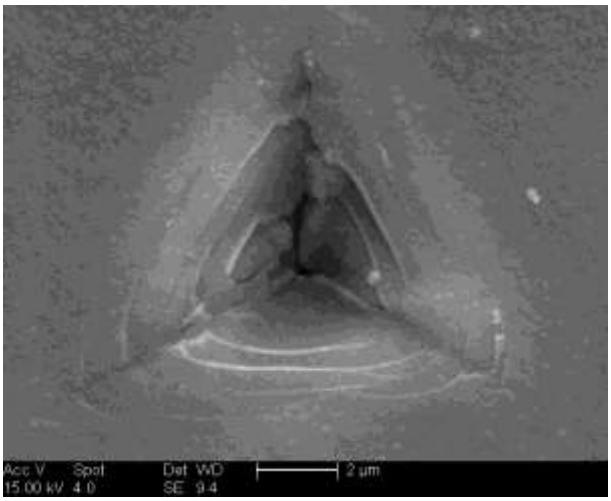

Figure 10a SEM micrograph of a 500mN nanoindentation showing nested cracks within the indentation

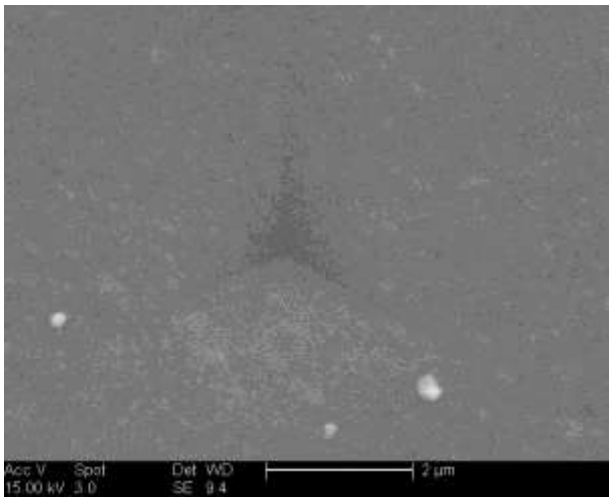

Figure 10b SEM micrograph of a 250mN nanoindentation showing little evidence of the indentation outline

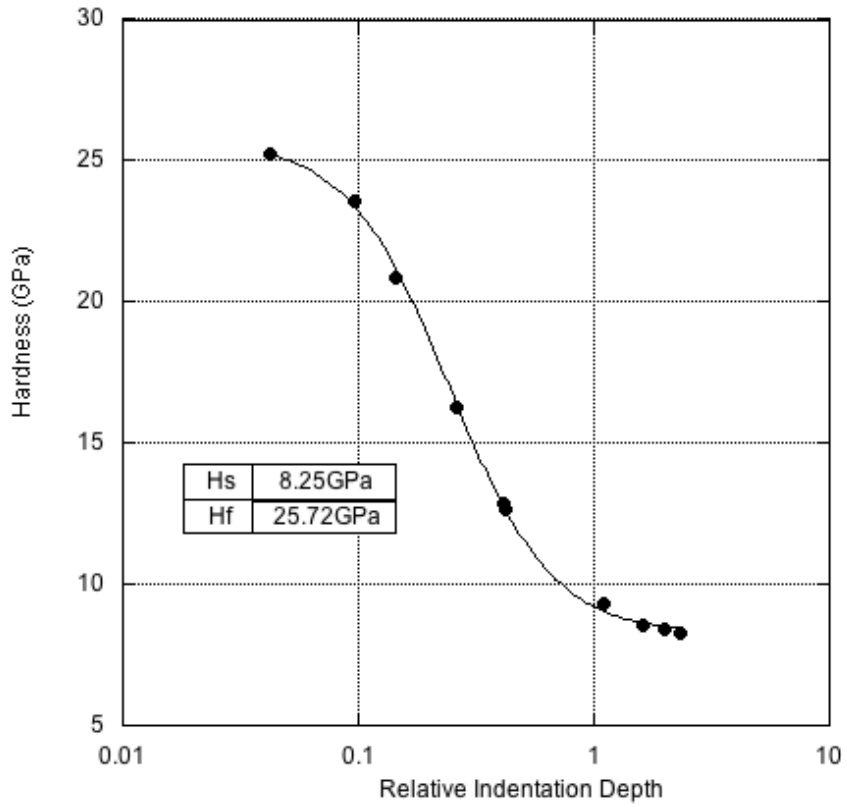

Figure 11: Hardness versus relative indentation depth for a PACVD a-C:H DLC coating. The data was fit by the Korsunsky model[76] to extract values for the substrate (H_s) and coating (H_f) hardness.

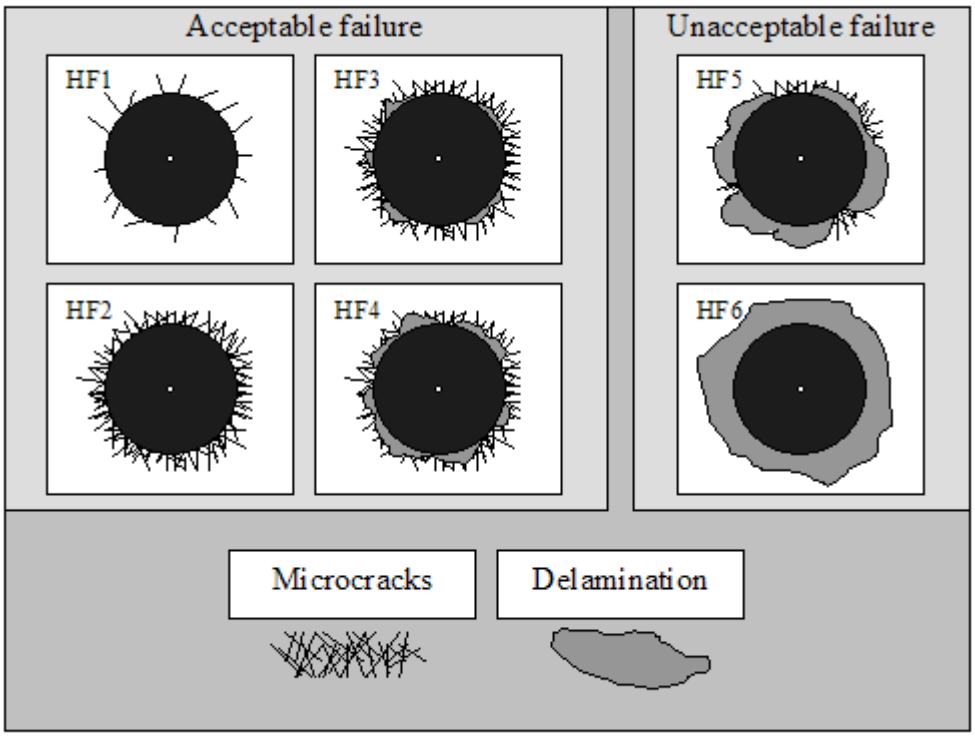

Figure 12: Schematic showing the acceptable and unacceptable failure morphologies around Rockwell indentations for the VDI 3198 adhesion test. Acceptable failures indicate a good level of adhesion between the coating and substrate[78]

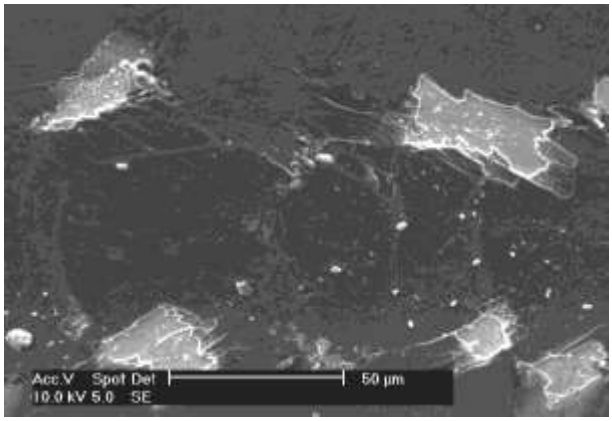

Figure 13a: Forward chevron cracking in a DLC coating on a nitrided steel substrate (scratch direction right to left)

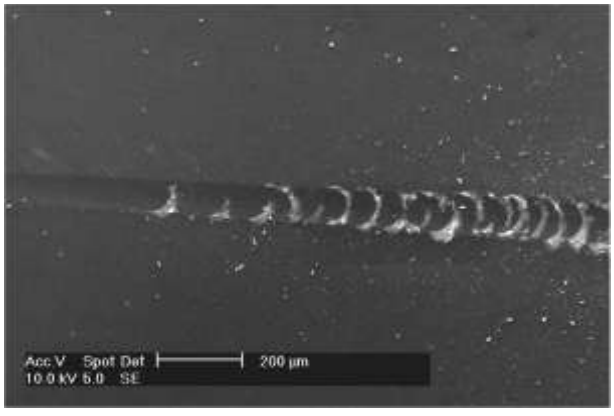

Figure 13b: Wedge spallation in a DLC coating on a steel substrate (scratch direction left to right)

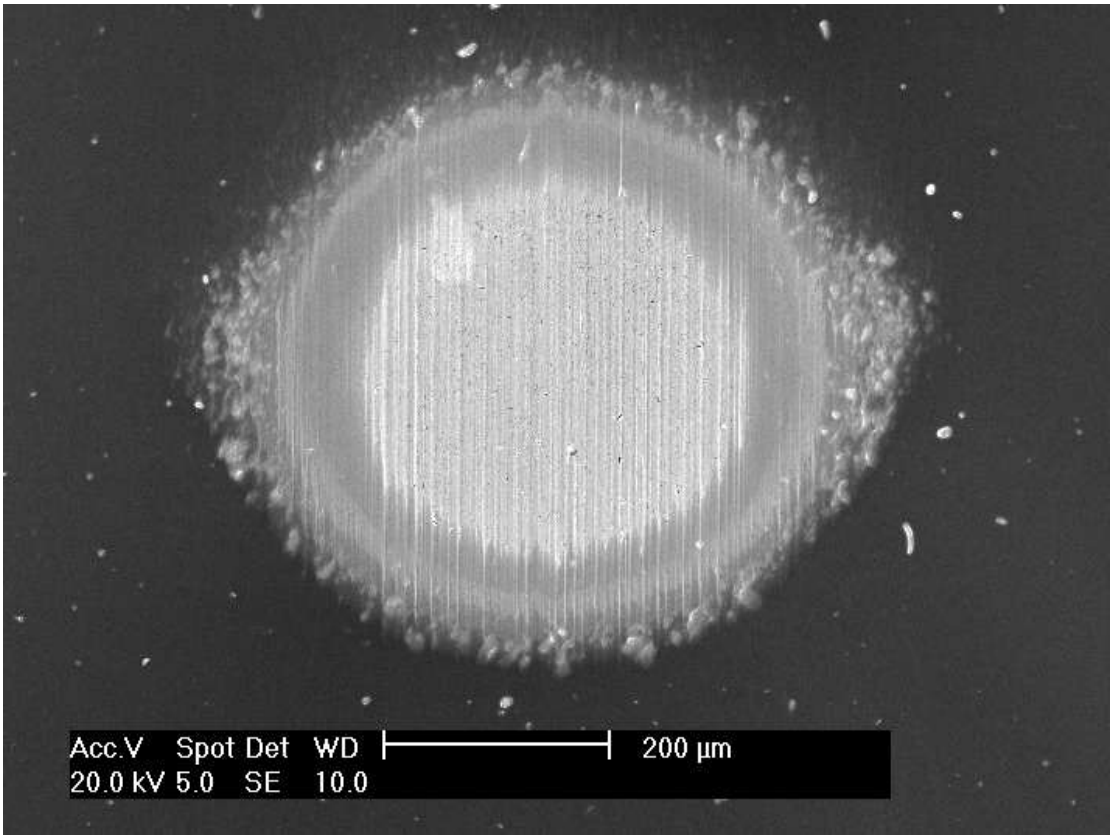

Figure 14: A microabrasion wear scar on an a-|C:H coating with TiN and SiC bond layers on a steel substrate . The different layers are clearly revealed and microabrasion wear testing can be used to measure the layer thicknesses and wear rate of the differing layers.

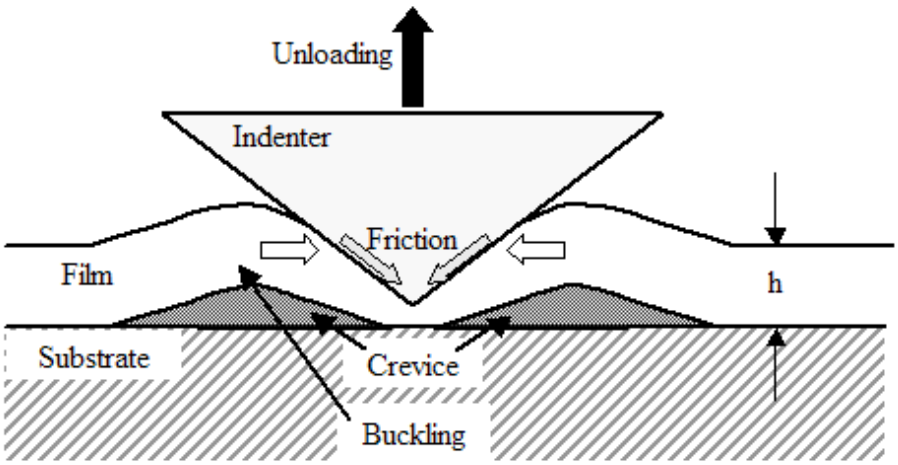

Figure 15: Schematic diagram showing the cracks introduced during a nanoindentation test that can be used for determining the fracture toughness of DLC coatings[100]

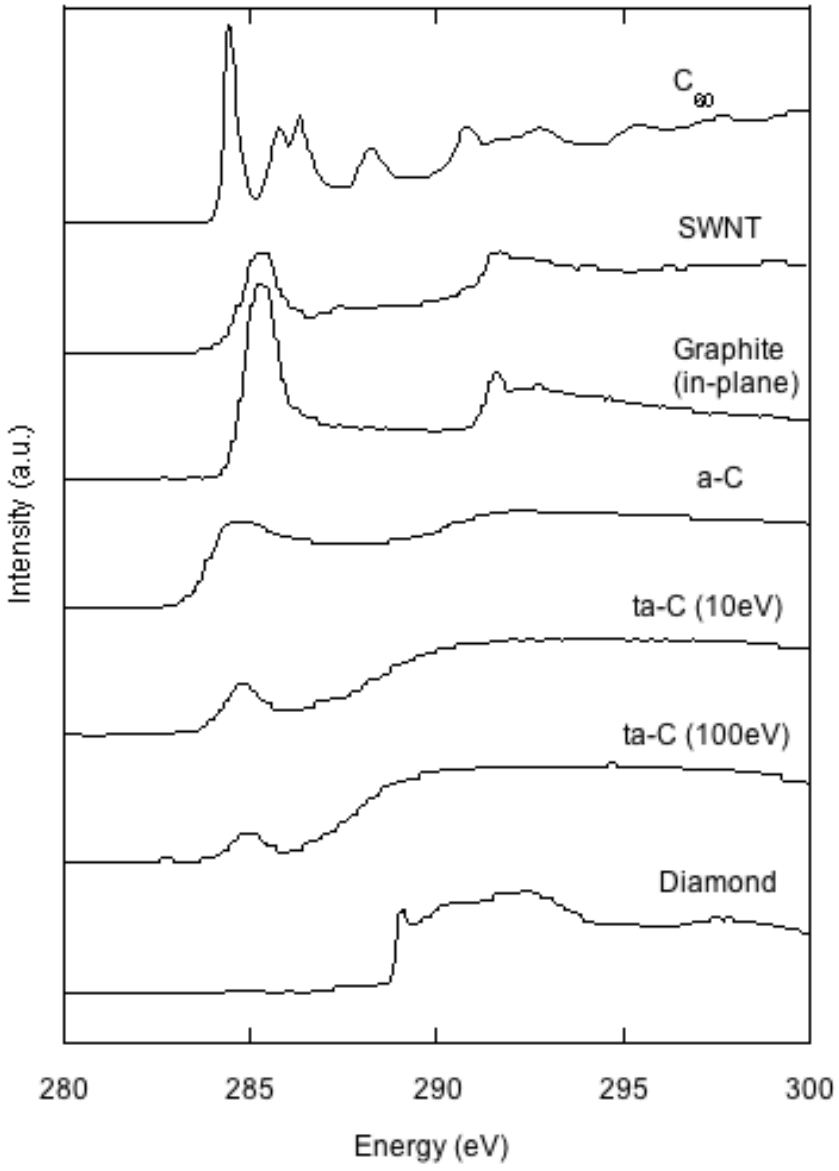

Figure 16: Schematic diagram showing EELS intensity versus energy for different types of carbon.[26] Plots of this type can be used to determine the sp^2/sp^3 bonding fractions in DLC films

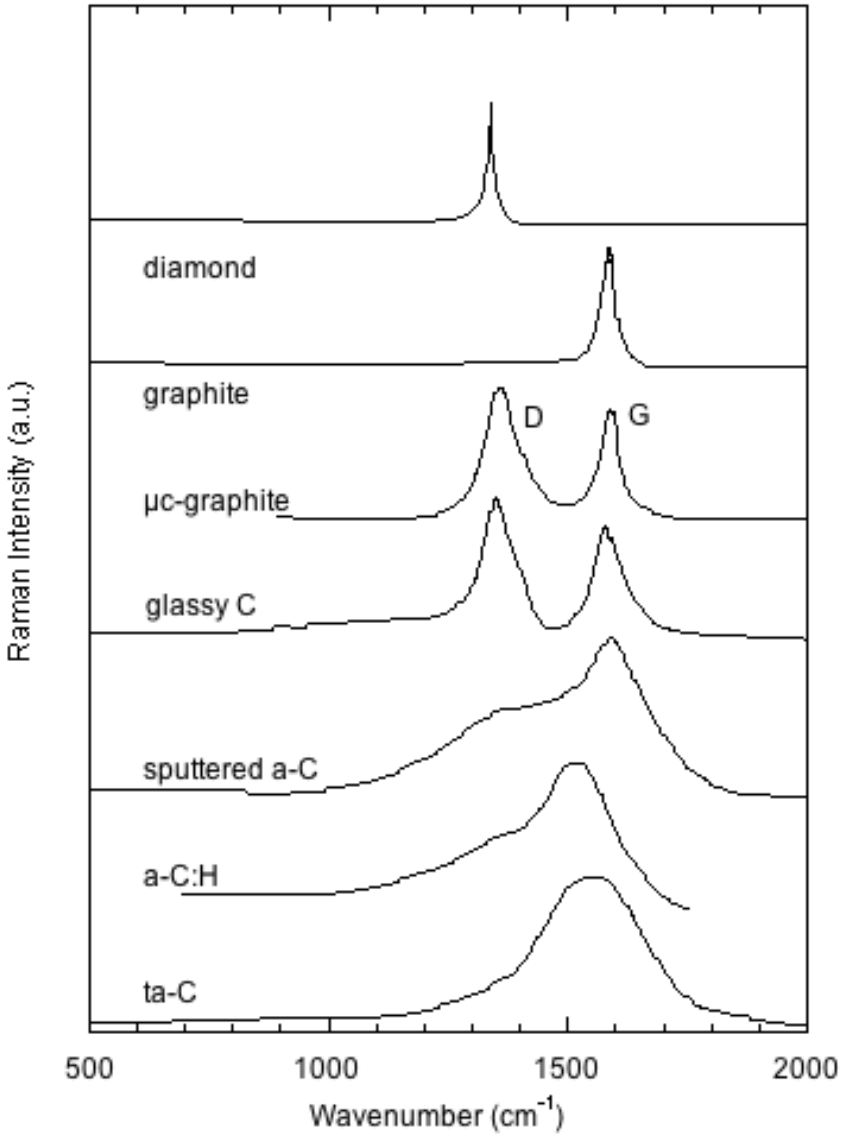

Figure 17: A typical Raman plot for different types of carbon.[26] Plots of this type can be used to determine sp^2/sp^3 fractions. The magnitude of peak shift can also be used to determine residual stress levels in the film

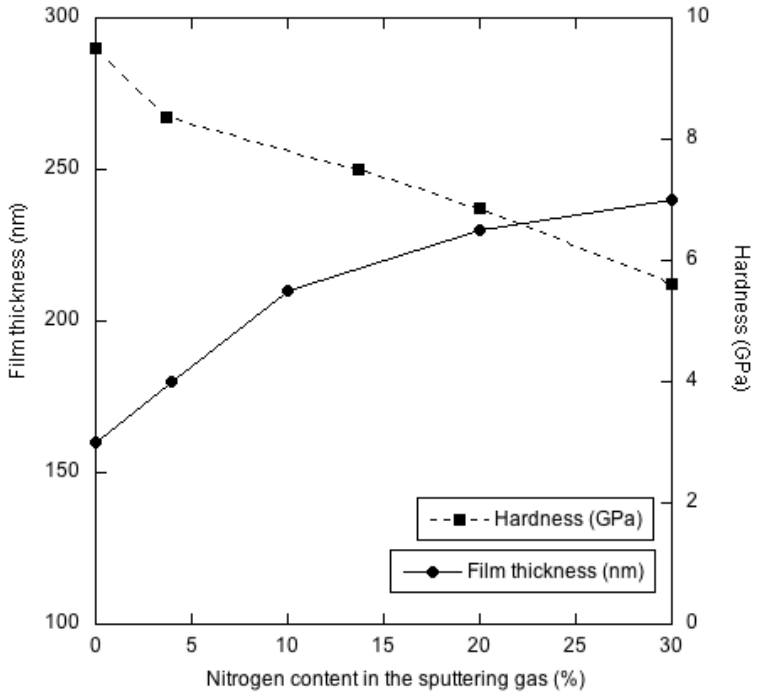

Figure 18: Film hardness and thickness as a function of nitrogen content[130]

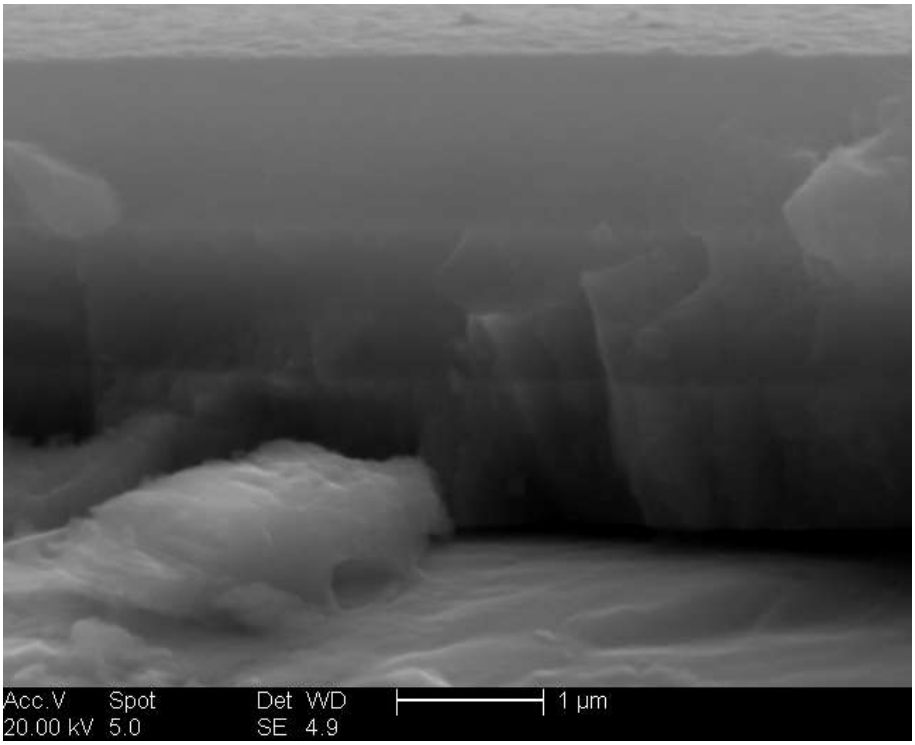

Figure 19: Cross-section through an a-C:H coating that clearly reveals three different layers, an a-C:H topcoat, a SiC interlayer and a TiN layer for promoting adhesion to the steel substrate.

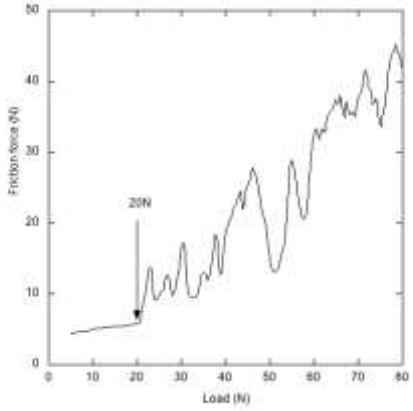

Figure 20a: DLC

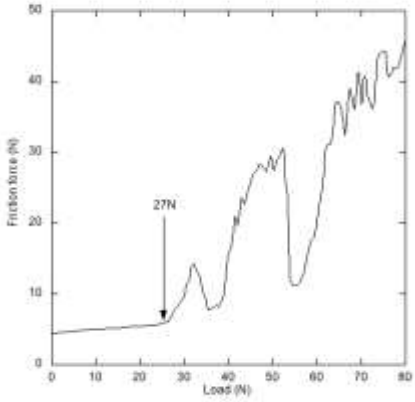

Figure 20b: DLC/Ti

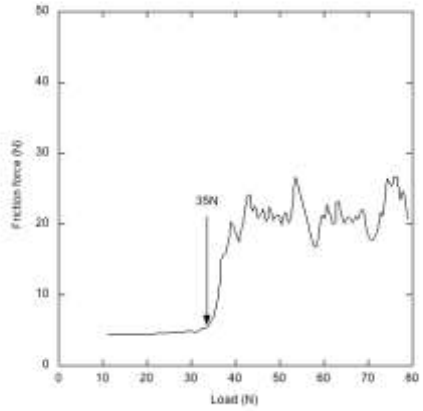

Figure 20c: DLC/TiN/Ti

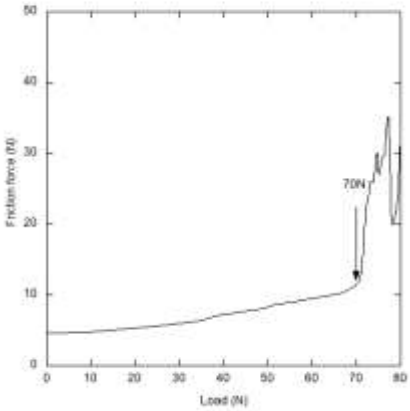

Figure 20d: DLC/Ti/TiN/TiCN

Figure 20: Scratch test critical load as a function of differing Ti-based interlayers for a DLC coating on an M2 steel substrate[137]

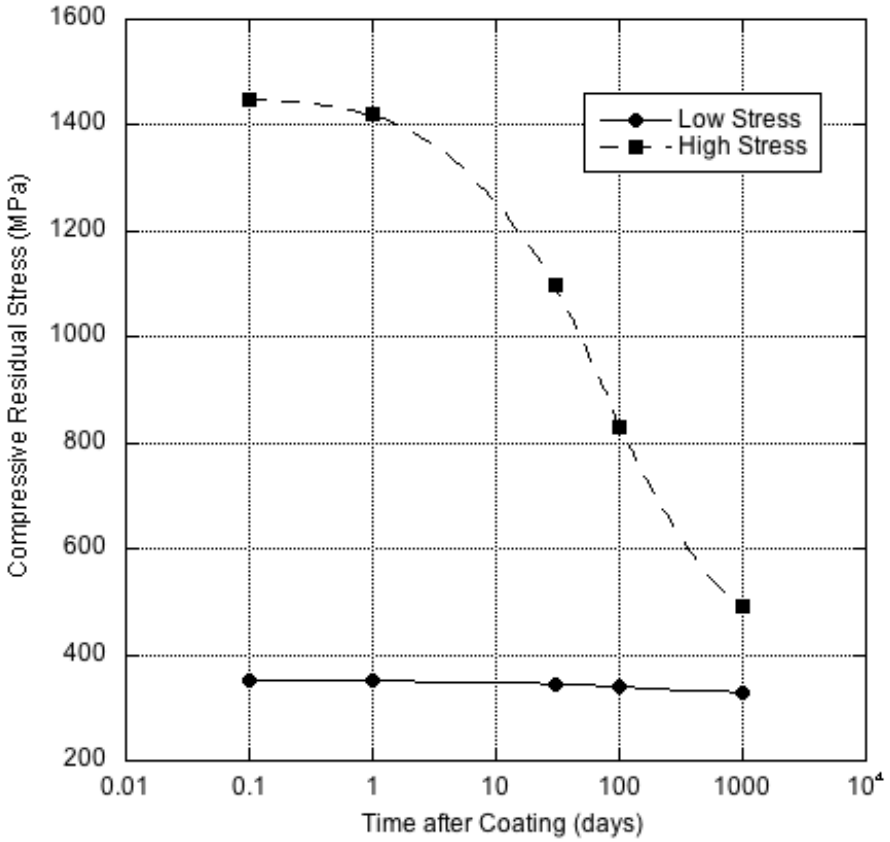

Figure 21: Effect of exposure time on the measured residual stress for 1 μm thick DLC films on silicon deposited by ion-beam-assisted deposition at AEA Technology using process parameters designed to generate low and high residual stresses[178]

Figure 22: Examples of razors with DLC-coated blades

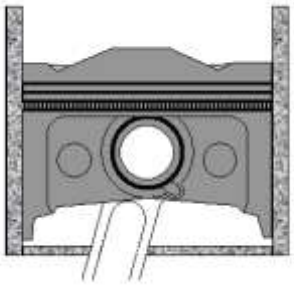

a) Piston

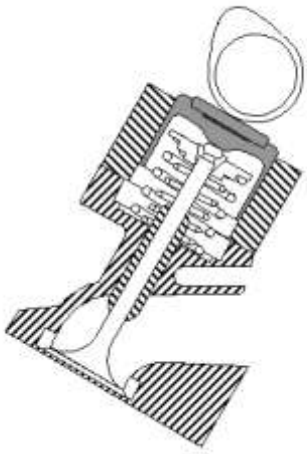

b) Tappet

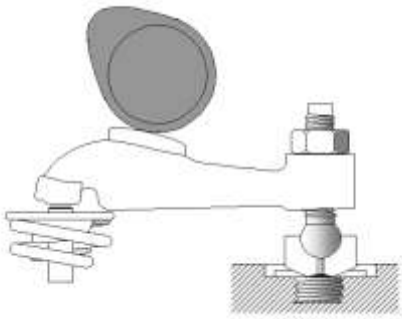

c) Camshaft

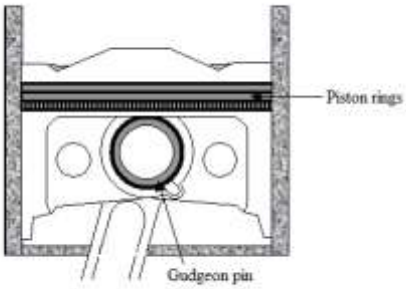

c) Piston rings and gudgeon pin

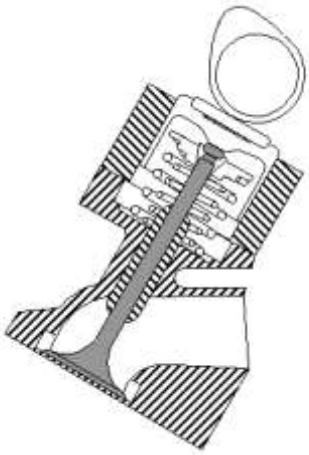

d) Valve stem and head

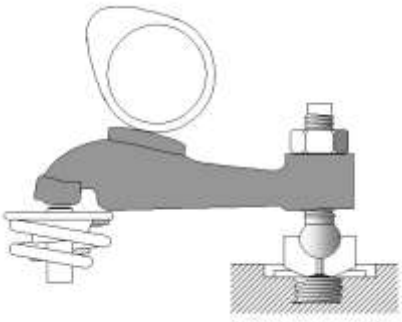

e) Rocker arm

Figure 23: Components that have been successfully coated with DLC for use in an automotive engine. Areas in solid grey are DLC coated.

Figure 24: A selection of automotive engine components that have been coated successfully with DLC (picture courtesy Bekaert).

	sp^3 content (%)	Hydrogen content (%)	Density ($g\ cm^{-3}$)	Poisson's ratio	Young's modulus (GPa)	Fracture toughness MPa√m	Residual stress (GPa)	Hardness (GPa)	References
Diamond	100	0	3.515	0.07	1144	3.4	-	100	[4]
Graphite	0	0	2.267	0.2	9-15	-	-	0.2	[5]
a-C:H (hard)	40	30-40	1.6-2.2	0.4	140-170	1.2-1.6	1-3	10-20	[6-8]
a-C:H (soft)	60	40-50	1.2-1.6	0.25	50	2.9-3.3	~1	<10	[6, 8, 9]
ta-C	80-88	0	3.1	0.12	757 ± 47.5	-	<12	40-90	[10, 11]
ta-C:H	70	30	2.35	0.3 ± 0.09	300 ± 49	-	8.4	≤50	[10-12]
W-DLC	~50	20%	2.5-16.3	0.2	100-150	1.0-2.5	0.9	13.2	[13-19]
Si-DLC	60-84	15	1.85	-	100-175	-	1-2.5	14-25	[20-25]

Table 1: Properties of various amorphous carbon films in comparison with diamond and graphite.

REFERENCES

1. Aisenberg, S. and F.M. Kimock, Materials Science Forum, 1989. **52/53**: p. 1-40.
2. Buffone, C., et al., *Heat transfer enhancement in heat pipe applications using surface coating.* Journal of Enhanced Heat Transfer, 2005. **12**(1): p. 21-35.
3. Schlatter, M., *DLC-based wear protection on magnetic storage media.* Diamond and Related Materials, 2002. **11**: p. 1781-1787.
4. Field, J.E., *Properties of Diamond*. 1993, London: Academic Press.
5. Bhushan, B., *Handbook Of Tribology*.
6. Jiang, X., K. Reichelt, and B. Stritzker, *The hardness and Young's modulus of a-C:H films.* Vacuum, 1990. **41**(4-6): p. 1381-1382.
7. Kodali, P., K.C. Walter, and M. Nastasi, *Investigation of mechanical and tribological properties of amorphous diamond-like carbon coatings.* Tribology International, 1997. **30**(8): p. 591-598.
8. Koidl, P., et al., *Plasma deposition, properties and structure of amorphous hydrogenated carbon films.* Mater. Sci. Forum, 1989. **52&53**: p. 41.
9. Michel, M.D., et al., *Fracture toughness, hardness and elastic modulus of hydrogenated amorphous carbon films deposited by chemical vapor deposition.* Thin Solid Films, 2006. **496**(2): p. 481-488.
10. Ferrari, A.C., et al., Appl. Phys. Lett., 1999. **75**: p. 1893.
11. *Verein Deutscher Ingenieure Normen, VDI 2840, VDI-Verlag, Dusseldorf.* 2005.
12. Pastorelli, R., et al., *Elastic constants of ultrathin diamond-like carbon films.* Diamond and Related Materials, 2000. **9**(3-6): p. 825-830.
13. Jiang, X., J. Fassbender, and B. Hillebrands, *Elastic constants of WC-a-C:H composite films studied by Brillouin spectroscopy.* Physical Review B, 1994. **49**(19): p. 13815 LP - 13819.
14. Cho, S.-J., et al., *Determination of elastic modulus and Poisson's ratio of diamond-like carbon films.* Thin Solid Films, 1999. **341**(1-2): p. 207-210.
15. Wang, J.S., et al., *The mechanical performance of DLC films on steel substrates.* Thin Solid Films, 1998. **325**(1-2): p. 163-174.
16. Cooper, C.V., et al., *Spectroscopic and selected mechanical properties of diamond-like carbon films synthesized by broad-beam ion deposition from methane.* Diamond and Related Materials, 1994. **3**(4-6): p. 534-541.
17. Cooper, C.V., P. Holiday, and A. Matthews, *The effect of TiN interlayers on the indentation behavior of diamond-like carbon films on alloy and compound substrates.* Surface and Coatings Technology, 1994. **63**(3): p. 129-134.
18. Harry, E., et al., *Mechanical properties of W and W(C) thin films: Young's modulus, fracture toughness and adhesion.* Thin Solid Films, 1998. **332**(1-2): p. 195-201.
19. Kalin, M. and J. Vizintin, *A comparison of the tribological behaviour of steel/steel, steel/DLC and DLC/DLC contacts when lubricated with mineral and biodegradable oils.* Wear Papers presented at the 11th Nordic Symposium on Tribology, NORDTRIB 2004, 2006. **261**(1): p. 22-31.

20. Varma, A., V. Palshin, and E.I. Meletis, *Structure-property relationship of Si-DLC films.* Surface and Coatings Technology, 2001. **148**(2-3): p. 305-314.

21. Abbas, G.A., J.A. McLaughlin, and E. Harkin-Jones, *A study of ta-C, a-C:H and Si-a:C:H thin films on polymer substrates as a gas barrier.* Diamond and Related Materials, 2004. **13**(4-8): p. 1342-1345.

22. Ogwu, A.A., et al., *The influence of biological fluids on crack spacing distribution in Si-DLC films on steel substrates.* Acta Materialia, 2003. **51**(12): p. 3455-3465.

23. Damasceno, J.C., et al., *Deposition of Si-DLC films with high hardness, low stress and high deposition rates.* Surface and Coatings Technology, 2000. **133-134**: p. 247-252.

24. Damasceno, J.C., S.S. Camargo Jr, and M. Cremona, *Optical and mechanical properties of DLC-Si coatings on polycarbonate.* Thin Solid Films, 2003. **433**(1-2): p. 199-204.

25. Lee, K.-R., et al., *Structural dependence of mechanical properties of Si incorporated diamond-like carbon films deposited by RF plasma-assisted chemical vapour deposition.* Thin Solid Films, 1997. **308-309**: p. 263-267.

26. Robertson, J., *Diamond-like amorphous carbon.* Materials Science and Engineering: R: Reports, 2002. **37**(4-6): p. 129-281.

27. Lifshitz, Y., *Diamond-like carbon -- present status.* Diamond and Related Materials, 1999. **8**(8-9): p. 1659-1676.

28. Pierson, H.O., *Handbook of Carbon, Graphite, Diamond and Fullerenes - Properties, Processing and Applications*. 1993: William Andrew Publishing/Noyes.

29. Wei, Q. and J. Naryan, *Superhard diamondlike carbon: preparation, theory and properties.* International Materials Reviews, 2000. **45**(4): p. 133-164.

30. Renevier, N.M., et al., *Performance of low friction MoS2/titanium composite coatings used in forming applications.* Materials & Design, 2000. **21**(4): p. 337-343.

31. Kaufman, H.R., *Broad-beam ion sources: Present status and future directions.* Journal of Vacuum Science & Technology A: Vacuum, Surfaces, and Films, 1986. **4**(3): p. 764-771.

32. Xu, S., L.K. Cheah, and B.K. Tay, *Spectroscopic ellipsometry studies of tetrahedral amorphous carbon prepared by filtered cathodic vacuum arc technique.* Thin Solid Films, 1998. **312**(1-2): p. 160-169.

33. Sanders, D.M. and E.A. Pyle, *Magnetic enhancement of cathodic arc deposition.* Journal of Vacuum Science & Technology A: Vacuum, Surfaces, and Films, 1987. **5**(4): p. 2728-2731.

34. X. Shi, et al., Philos. Mag. B, 1997. **76**: p. 351.

35. X. Shi, B.K. Tay, and S.P. Lau., Int. J. Mod. Phys., 2000. **14**: p. 154.

36. Anders, S., et al., *S-shaped magnetic macroparticle filter for cathodic arc deposition.* IEEE Transactions on Plasma Science, 1997. **25**(4): p. 670-674.

37. Anders, A., *Approaches to rid cathodic arc plasmas of macro- and nanoparticles: a review.* Surface and Coatings Technology, 1999. **120-121**: p. 319-330.

38. A. Anders and A. Kulkarni, Mater. Res. Soc. Symp. Proc., 2001. **675**: p. W11.1.

39. Polo, M.C., et al., *Preparation of tetrahedral amorphous carbon films by filtered cathodic vacuum arc deposition.* Diamond and Related Materials, 2000. **9**(3-6): p. 663-667.

40. Coll, B.F., *Amorphous Carbon*, in *Worid Scientific*, e.a. S.R.P. Silva, Editor. 1998: Singapore.

41. McKenzie, D.R., *Tetrahedral bonding in amorphous carbon.* Reports on Progress in Physics, 1996. **59**(12): p. 1611-1664.

42. Gupta, B.K. and B. Bhushan, *Micromechanical properties of amorphous carbon coatings deposited by different deposition techniques.* Thin Solid Films, 1995. **270**(1-2): p. 391-398.

43. Anders, S., et al., *Effect of vacuum arc deposition parameters on the properties of amorphous carbon thin films.* Surface and Coatings Technology, 1994. **68-69**: p. 388-393.

44. Voevodin, A.A. and M.S. Donley, *Preparation of amorphous diamond-like carbon by pulsed laser deposition: a critical review.* Surface and Coatings Technology, 1996. **82**(3): p. 199-213.

45. Kim, Y.T., et al., *Dependence of the bonding structure of DLC thin films on the deposition conditions of PECVD method.* Surface and Coatings Technology, 2003. **169-170**: p. 291-294.

46. Yang, W.J., et al., *Microstructure and tribological properties of SiOx/DLC films grown by PECVD.* Surface and Coatings Technology, 2005. **194**(1): p. 128-135.

47. Fedosenko, G., et al., *Pulsed PECVD deposition of diamond-like carbon films.* Diamond and Related Materials, 2002. **11**(3-6): p. 1047-1052.

48. Bremond, F., P. Fournier, and F. Platon, *Test temperature effect on the tribological behavior of DLC-coated 100C6-steel couples in dry friction.* Wear, 2003. **254**(7-8): p. 774-783.

49. Platon, F., P. Fournier, and S. Rouxel, *Tribological behaviour of DLC coatings compared to different materials used in hip joint prostheses.* Wear, 2001. **250**(1-12): p. 227-236.

50. Page, T.F. and S.V. Hainsworth, *Using Nanoindentation Techniques for the Characterisation of Coated Systems: A Critique.* Surface and Coatings Technology, 1993. **61**: p. 201-208.

51. Yu, H.Y., S.C. Sanday, and B.B. Rath, *The effect of substrate on the elastic properties of films determined by the indentation test - axisymmetric Boussinesq problem.* J. Mech. Phys. Solids, 1990. **38**(6): p. 745-764.

52. Saha, R. and W.D. Nix, *Effects of the substrate on the determination of thin film mechanical properties by nanoindentation.* Acta Materialia, 2002. **50**: p. 23-28.

53. Hainsworth, S.V., H.W. Chandler, and T.F. Page, *Mechanical Property Data for Coated Systems - the Prospects for Measuring "Coating Only" Properties using Nanoindentation.* Mat. Res. Soc. Symp. Proc., 1997. **436**: p. 171-176.

54. Oliver, W.C. and G.M. Pharr, *An improved technique for determining hardness and elastic modulus using load and displacement sensing indentation experiments.* J. Materials Research, 1992. **7**: p. 1564-1583.

55. Doerner, M.F. and W.D. Nix, *A method for interpreting the data from depth-sensing indentation instruments.* J. Materials Research, 1986. **1**: p. 601-609.

56. Pharr, G.M., W.C. Oliver, and F.R. Brotzen, *On the Generality of the Relationship among Contact Stiffness, Contact Area, and Elastic Modulus during Indentation.* J. Materials Research, 1992. **7**: p. 613-617.

57. Sneddon, I., *The relation between load and penetration in the axisymmetric Boussinesq problem for a punch of arbitrary profile.* International Journal Engineering Science, 1965. **3**: p. 47-57.

58. Tabor, D., *The Hardness of Metals*. Oxford Classic Texts in the Physical Sciences. 2000: Oxford University Press.

59. Meyer, E., Zeitschrift des Vereines Deutscher Ingenieure 1908. **52**: p. 645, 740, 835.

60. *ISO/FDIS 14577-1, Metallic materials - Instrumented indentation test for hardness and materials parameters - Part1: Test method*.

61. Xu, Z.-H. and D. Rowcliffe, *Nanoindentation of diamond-like carbon and alumina coatings.* Surface and Coatings Technology, 2002. **161**: p. 44-51.

62. Hainsworth, S.V., T. Bartlett, and T.F. Page, *The Nanoindentation Response of Systems with Thin Hard Carbon Coatings.* Thin Solid Films, 1993. **236**: p. 214-218.

63. Zhang, T.H. and Y. Huan, *Nanoindentation and nanoscratch behaviors of DLC coatings on different steel substrates.* Composites Science and Technology, 2005. **65**(9): p. 1409-1413.

64. Lee, Y.-H., K. Takashima, and D. Kwon, *Micromechanical analysis on residual stress-induced nanoindentation depth shifts in DLC films.* Scripta Materialia, 2004. **50**(9): p. 1193-1198.

65. Bruno, P., et al., *Mechanical properties of PECVD hydrogenated amorphous carbon coatings via nanoindentation and nanoscratching techniques.* Surface and Coatings Technology, 2004. **180-181**: p. 259-264.

66. Jian, S.-R., T.-H. Fang, and D.-S. Chuu, *Nanoindentation investigation of amorphous hydrogenated carbon thin films deposited by ECR-MPCVD.* Journal of Non-Crystalline Solids, 2004. **333**(3): p. 291-295.

67. Logothetidis, S., et al., *Nanoindentation studies of multilayer amorphous carbon films.* Carbon, 2004. **42**(5-6): p. 1133-1136.

68. Takai, O., et al., *Nanoindentation studies on amorphous carbon nitride thin films prepared by shielded arc ion plating.* Surface and Coatings Technology, 2001. **142-144**: p. 719-723.

69. Martinez, E., et al., *Study of the mechanical properties of tetrahedral amorphous carbon films by nanoindentation and nanowear measurements.* Diamond and Related Materials, 2001. **10**(2): p. 145-152.

70. Charitidis, C., S. Logothetidis, and P. Douka, *Nanoindentation and nanoscratching studies of amorphous carbon films.* Diamond and Related Materials, 1999. **8**(2-5): p. 558-562.

71. Li, X., D. Diao, and B. Bhushan, *Fracture mechanisms of thin amorphous carbon films in nanoindentation.* Acta Materialia, 1997. **45**(11): p. 4453-4461.

72. Wright, T. and T.F. Page, *Nanoindentation and Microindentation Studies of Hard Carbon On 304 Stainless-Steel.* Surface & Coatings Technology, 1992. **55**(1-3): p. 557-562.

73. Meunier, F., *Modélisation des mécanismes de croissance des couches minces de carbone dur amorphe obtenues par CVD assistée plasma*. 1996, University of Limoges.

74. Jonsson, B. and S. Hogmark, *Hardness measurements of thin films.* Thin Solid Films, 1984. **114**(3): p. 257-269.

75. Burnett, P.J. and D.S. Rickerby, *The mechanical properties of wear-resistant coatings : I: Modelling of hardness behaviour.* Thin Solid Films, 1987. **148**(1): p. 41-50.

76. Korsunsky, A.M., et al., *On the hardness of coated systems.* Surface and Coatings Technology, 1998. **99**(1-2): p. 171-183.

77. Volinsky, A.A., N.R. Moody, and W.W. Gerberich, *Interfacial toughness measurements for thin films on substrates.* Acta Materialia, 2002. **50**(3): p. 441-466.

78. *Verein Deutscher Ingenieure Normen, VDI 3198, VDI-Verlag, Dusseldorf.* 1991.

79. Bull, S.J., *Failure mode maps in the thin film scratch adhesion test.* Tribology International, 1997. **30**(7): p. 491-498.

80. Santner, E., D. Klaffke, and G. Meier zu Kocker, *Comprehensive tribological characterization of thin TiN-based coatings.* Wear, 1995. **190**(2): p. 204-211.

81. Ronkainen, H., et al., *Comparative tribological and adhesion studies of some titanium-based ceramic coatings.* Surface and Coatings Technology, 1990. **43-44**(Part 2): p. 888-897.

82. Erdemir, A. and G.R. Fenske, *Tribological performance of diamond and diamondlike carbon films at elevated temperatures.* Tribology Transactions, 1996. **39**(4): p. 787-794.

83. Shum, P.W., et al., *Mechanical and tribological properties of amorphous carbon films deposited on implanted steel substrates.* Thin Solid Films, 2004. **458**(1-2): p. 203-211.

84. Almond, E.A., L.A. Lay, and M.G. Gee. in *2nd International Conference on the Science of Hard Materials*. 1986.

85. Bull, S.J., et al., *The use of scratch adhesion testing for the determination of interfacial adhesion: The importance of frictional drag.* Surface and Coatings Technology, 1988. **36**(1-2): p. 503-517.

86. Kassman, A., et al., *A new test method for the intrinsic abrasion resistance of thin coatings.* Surface and Coatings Technology, 1991. **50**(1): p. 75-84.

87. Rutherford, K.L. and I.M. Hutchings, *A micro-abrasive wear test, with particular application to coated systems.* Surface and Coatings Technology, 1996. **79**(1-3): p. 231-239.

88. Rutherford, K.L. and I.M. Hutchings, *Theory and Application of a Micro-Scale Abrasive Wear Test.* Journal of Testing and Evaluation, 1997. **25**: p. 250-260.

89. Trezona, R.I., D.N. Allsopp, and I.M. Hutchings, *Transitions between two-body and three-body abrasive wear: influence of test conditions in the microscale abrasive wear test.* Wear, 1999. **225-229**(Part 1): p. 205-214.

90. Allsopp, D.N., R.I. Trezona, and I.M. Hutchings, *The effects of ball surface condition in the microâ€• scale abrasive wear test.* Tribology Letters, 1998. **5**(4): p. 259-264.

91. Gee, M.G. and M.J. Wicks, *Ball crater testing for the measurement of the unlubricated sliding wear of wear-resistant coatings.* Surface and Coatings Technology, 2000. **133-134**: p. 376-382.

92. Gåhlin, R., et al., *The crater grinder method as a means for coating wear evaluation -- an update.* Surface and Coatings Technology, 1997. **90**(1-2): p. 107-114.

93. Gee, M.G., et al., *Progress towards standardisation of ball cratering.* Wear, 2003. **255**(1-6): p. 1-13.

94. Kusano, Y. and I.M. Hutchings, *Sources of variability in the free-ball micro-scale abrasion test.* Wear, 2005. **258**(1-4): p. 313-317.

95. Hollman, P., et al., *Tribological evaluation of thermally activated CVD diamond-like carbon (DLC) coatings.* Surface and Coatings Technology, 1997. **96**(2-3): p. 230-235.

96. Dorner, A., et al., *Diamond-like carbon-coated Ti6Al4V: influence of the coating thickness on the structure and the abrasive wear resistance.* Wear, 2001. **249**(5-6): p. 489-497.

97. Bandorf, R., et al., *Influence of substrate material and topography on the tribological behaviour of submicron coatings.* Surface and Coatings Technology, 2003. **174-175**: p. 461-464.

98. Nastasi, M., et al., *Fracture toughness of diamond-like carbon coatings.* J. Mater. Res, 1999. **14**(5): p. 2173-2180.

99. Anstis, G.R., et al., *A critical review of indentation techniques for measuring fracture toughness; I, Direct Crack Measurements.* J. Amer. Ceram. Soc., 1981. **64**: p. 533-543.

100. Lin, J.F., et al., *Effect of nitrogen content at coating film and film thickness on nanohardness and Young's modulus of hydrogenated carbon films.* Diamond and Related Materials, 2004. **13**(1): p. 42-53.

101. Ferrari, A.C., et al., *Density, sp3 fraction and cross-sectional structure of amorphous carbon films determined by x-ray reflectivity and electron energy-loss spectroscopy.* Phys. Rev. B, 2000. **62**(16): p. 11089-11103.

102. Berger, S.D., D.R. McKenzie, and P.J. Martin, *EELS analysis of vacuum arc-deposited diamond-like films.* Philosophical Magazine Letters, 1988. **57**(6): p. 285-290.

103. Prawer, S., et al., *Systematic variation of the Raman spectra of DLC films as a function of sp2:sp3 composition.* Diamond and Related Materials, 1996. **5**(3-5): p. 433-438.

104. Gilkes, K.W.R., et al., *Direct quantitative detection of the sp(3) bonding in diamond-like carbon films using ultraviolet and visible Raman spectroscopy.* Journal of Applied Physics, 2000. **87**: p. 7283-7289.

105. Racine, B., et al., *Properties of amorphous carbon-silicon alloys deposited by a high plasma density source.* J. Appl. Phys., 2001. **90**(10): p. 5002-5012.

106. Ferrari, A.C. and J. Robertson, *Resonant Raman spectroscopy of disordered, amorphous, and diamondlike carbon.* Phys. Rev. B, 2001. **64**(7): p. Art no. 075414.

107. Donnet, C., et al., *Solid state C and H nuclear magnetic resonance investigations of hydrogenated amorphous carbon.* Journal of Applied Physics, 1999. **85**(6): p. 3264-3270.

108. Golzan, M.M., et al., *NMR evidence for strained carbon bonding in tetrahedral amorphous carbon.* Chemical Physics, 1995. **193**(1-2): p. 167-172.

109. Grill, A., et al., *Inhomogeneous carbon bonding in hydrogenated amorphous carbon films.* Journal of Applied Physics, 1987. **61**(8, Part 1): p. 2874-2877.

110. Jager, C., et al., *Structural properties of amorphous hydrogenated carbon. III. NMR investigations.* Physical Review B (Condensed Matter), 1994. **50**(2): p. 846-852.

111. Jarman, R.H., et al., *Determination of bonding in amorphous carbon films: a quantitative comparison of core-electron energy-loss spectroscopy and C nuclear magnetic resonance spectroscopy.* Applied Physics Letters, 1986. **49**(17): p. 1065-1067.

112. Kaplan, S., F. Jansen, and M. Machonkin, *Characterization of amorphous carbon-hydrogen films by solid-state nuclear magnetic resonance.* Applied Physics Letters, 1985. **47**(7): p. 750-753.

113. Kleber, R., et al., *Characterization of the sp2 bonds network in a-C:H layers with nuclear magnetic resonance, electron energy loss spectroscopy and electron spin resonance.* Thin Solid Films, 1991. **205**(2): p. 274-278.

114. Mauri, F., B.G. Pfrommer, and S.G. Louie, *Ab initio NMR chemical shift of diamond, chemical-vapor-deposited diamond, and amorphous carbon.* Physical Review Letters, 1997. **79**(12): p. 2340-2343.

115. Pan, H., et al., Phys. Rev., 1991. **B**(44): p. 6741-6745.

116. Tamor, M.A., W.C. Vassell, and K.R. Carduner, *Atomic constraint in hydrogenated 'diamond-like' carbon.* Applied Physics Letters, 1991. **58**(6): p. 592-594.

117. Stoney, G.G., *The tension of metallic films deposited by electrolysis.* Proc. Roy. Soc. (London), 1909. **A82**: p. 172-175.

118. Sergo, V., O. Sbaizero, and D.R. Clarke, *Mechanical and chemical consequences of the residual stresses in plasma sprayed hydroxyapatite coatings.* Biomaterials, 1997. **18**(6): p. 477-482.

119. Kleinsorge, B., et al., *Hydrogen and disorder in diamond-like carbon.* Diamond and Related Materials, 2001. **10**(3-7): p. 965-969.

120. Erdemir, A., *The role of hydrogen in tribological properties of diamond-like carbon films.* Surface and Coatings Technology, 2001. **146-147**: p. 292-297.

121. Ronkainen, H., et al., *Differentiating the tribological performance of hydrogenated and hydrogen-free DLC coatings.* Wear, 2001. **249**(3-4): p. 260-266.

122. Pepper, S.V., J. Vac. Sci. Technol., 1982. **20**: p. 643-.

123. Kim, D.S., T.E. Fischer, and B. Gallois, *The effects of oxygen and humidity on friction and wear of diamond-like carbon films.* Surface and Coatings Technology, 1991. **49**(1-3): p. 537-542.

124. Gardos, M.N., Surface and Coatings Technology, 1999. **113**: p. 183.

125. Donnet, C., et al., Tribology Letters, 1998. **4**: p. 259-.

126. Donnet, C., Surface and Coatings Technology, 1998. **100-101**: p. 180.

127. Erdemir, A., *Genesis of superlow friction and wear in diamondlike carbon films.* Tribology International, 2004. **37**(11-12): p. 1005-1012.

128. Erdemir, A., et al., *Synthesis of superlow-friction carbon films from highly hydrogenated methane plasmas.* Surface and Coatings Technology, 2000. **133-134**: p. 448-454.

129. Jones, A.H.S., et al., *Novel high wear resistant diamond-like carbon coatings deposited by magnetron sputtering of carbon targets.* Proc. Instn. Mech. Eng. Part J, 1998. **212**: p. 301-306.

130. Guerino, M., et al., *The influence of nitrogen on the dielectric constant and surface hardness in diamond-like carbon (DLC) films.* Diamond and Related Materials, 2004. **13**(2): p. 316-319.

131. Robertson, J., *Deposition mechanism of diamond-like a-C and a-C:H.* Diamond and Related Materials, 1994. **3**(4-6): p. 361-368.

132. Sugimoto, I. and S. Miyake, *Oriented hydrocarbons transferred from a high performance lubricative amorphous C:H:Si film during sliding in a vacuum.* Appl. Phys. Lett., 1990. **56**: p. 1868-1870.

133. Miyake, S., *Tribological Properties of Hard Carbon-Films - Extremely Low Friction Mechanism of Amorphous Hydrogenated Carbon-Films and Amorphous Hydrogenated SiC Films in Vacuum.* Surface and Coatings Technology, 1992. **55**: p. 563-569.

134. Oguri, K. and T. Arai, *Two different low friction mechanisms of diamond-like carbon with silicon coatings formed by plasma-assisted chemical vapour deposition.* J. Mater. Res, 1992. **7**: p. 1313-1316.

135. Oguri, K. and T. Arai, *Tribological properties and characterisation of DLC coatings with silicon prepared by plasma-assisted chemical vapour deposition.* Surface and Coatings Technology, 1991. **47**: p. 710-721.

136. Palshin, V., et al., *X-ray absorption spectroscopy, simulation and modeling of Si- DLC films.* Journal of Materials Science, 2002. **37**(8): p. 1535-1539.

137. Chang, C.-L. and D.-Y. Wang, *Microstructure and adhesion characteristics of diamond-like carbon films deposited on steel substrates.* Diamond and Related Materials, 2001. **10**(8): p. 1528-1534.

138. Oguri, K. and T. Arai, *Low friction coatings of diamond-like carbon with silicon prepared by plasma-assisted chemical vapor deposition.* Journal of Materials Research, 1990. **5**(11): p. 2567-2571.

139. Gangopadhyay, A., et al., *Amorphous hydrogenated carbon films for tribological applications I. Development of moisture insensitive films having reduced compressive stress.* Tribology International, 1997. **30**: p. 9-18.

140. Grill, A., V. Patel, and B.S. Meyerson, *Optical and tribological properties of heat-treated diamond-like carbon films.* J. Mater. Res, 1990. **5**: p. 2531-2537.

141. Memming, R., T. H.J., and P.E. Wierenga, *Properties of polymeric layers of hydrogenated amorphous-carbon produced by a plasma-activated chemical vapor-deposition process .2. Tribological and mechanical-properties.* Thin Solid Films, 1986. **143**: p. 31-41.

142. Kattamis, T.Z., S. Skolianos, and C.G. Fountzoulas, *Effect of annealing on the cohesion, adhesion and tribological behaviour of amorphous silicon containing diamond-like carbon (Si-DLC) coatings on steel.* J. Adhesion Science and Technology, 2000. **14**: p. 805-816.

143. Gilmore, R. and R. Hauert, *Comparitive study of the tribological moisture sensitivity of Si-free and Si-containing diamond-lie carbon films.* Surface & Coatings Technology, 2000. **133-134**: p. 437-442.

144. Gilmore, R. and R. Hauert, *Control of the tribological moisture sensitivity of diamond-like carbon films by alloying with F, Ti or Si.* Thin Solid Films, 2001. **398-399**: p. 199-204.

145. Meneve, J., et al., *Friction and wear behavior of amorphous hydrogenated Si1-xCx films.* Surface & Coatings Technology, 1993. **62**: p. 577-582.

146. Müller, U. and R. Hauert, *The coefficient of static friction of silicon containing diamond-like carbon films.* Surface & Coatings Technology, 2004. **177-178**: p. 552-557.

147. Fischer, T.E., *Tribochemistry.* Annual Review of Materials Science, 1988. **18**: p. 303-323.

148. Ban, M., et al., *Tribological characteristics of Si-containing diamond-like carbon films under oil-lubrication.* Wear, 2002. **253**(3-4): p. 331-338.

149. Wänstrand, O., M. Larsson, and P. Hedenqvist, *Mechanical and tribological evaluation of PVD WC/C coatings.* Surface and Coatings Technology, 1999. **111**: p. 247-254.

150. Podgornik, B. and J. Vizintin, *Influence of substrate treatment on the tribological properties of DLC coatings.* Diamond and Related Materials, 2001. **10**: p. 2232-2237.

151. Lindholm, P., S. Bjorklund, and F. Svahn, *Method and surface roughness aspects for the design of DLC coatings.* Wear Papers presented at the 11th Nordic Symposium on Tribology, NORDTRIB 2004, 2006. **261**(1): p. 107-111.

152. Baranov, A.M., *Planarization of substrate surface by means of ultrathin diamond-like carbon film.* Surface and Coatings Technology, 1998. **102**(1-2): p. 154-158.

153. Peng, X.L., Z.H. Barber, and T.W. Clyne, *Surface roughness of diamond-like carbon films prepared using various techniques.* Surface and Coatings Technology, 2001. **138**(1): p. 23-32.

154. Lifshitz, Y., *Hydrogen-free amorphous carbon films: Correlation between growth conditions and properties.* Diamond and Related Materials, 1996. **5**(3-5): p. 388-400.

155. Park, C., et al., *Electron emission characteristics of diamond like carbon films deposited by laser ablation technique.* Applied Surface Science, 1997. **111**: p. 140-144.

156. Hirakuri, K.K., et al., *Thin film characterization of diamond-like carbon films prepared by r.f. plasma chemical vapor deposition.* Thin Solid Films, 1997. **302**(1-2): p. 5-11.

157. Fung, M.K., et al., *Deposition of ultra-thin diamond-like carbon protective coating on magnetic disks by electron cyclotron resonance plasma technique.* Journal of Non-Crystalline Solids, 1999. **254**(1-3): p. 167-173.

158. Ali, A., K.K. Hirakuri, and G. Friedbacher, *Roughness and deposition mechanism of DLC films prepared by r.f. plasma glow discharge.* Vacuum, 1998. **51**(3): p. 363-368.

159. Zhang, Q., et al., *Deposition of hydrogenated diamond-like carbon films under the impact of energetic hydrocarbon ions.* Journal of Applied Physics, 1998. **84**(10): p. 5538-5542.

160. Maharizi, M., et al., *Physical properties of a:DLC films and their dependence on parameters of deposition and type of substrate.* Diamond and Related Materials, 1999. **8**(6): p. 1050-1056.

161. McNamara, B.P., H. Murphy, and M.M. Morshed, *Adhesion properties of diamond-like coated orthopaedic biomaterials.* Diamond and Related Materials, 2001. **10**(3-7): p. 1098-1102.

162. Berg, S., et al., *Influence of substrate material on the initial thin film growth during ion deposition from a glow discharge.* Vacuum, 1984. **34**(10-11): p. 969-973.

163. Sattel, S., et al., *Temperature dependence of the formation of highly tetrahedral a-C:H.* Diamond and Related Materials, 1996. **5**(3-5): p. 425-428.

164. Sattel, S., J. Robertson, and H. Ehrhardt, *Effects of deposition temperature on the properties of hydrogenated tetrahedral amorphous carbon.* Journal of Applied Physics, 1997. **82**(9): p. 4566-4576.

165. Rawles, R.E., et al., *Mechanism of surface smoothing of diamond by a hydrogen plasma.* Diamond and Related Materials, 1997. **6**(5-7): p. 791-795.

166. Salvadori, M.C., D.R. Martins, and M. Cattani, *DLC coating roughness as a function of film thickness.* Surface and Coatings Technology, 2006. **200**(16-17): p. 5119-5122.

167. Maharizi, M., et al., *Influence of Substrate and Film Thickness on The Morphology and Diamond Bond Formation During the Growth of Amorphous Diamond-like Carbon (DLC) Films.* Journal of Optoelectronics and Advanced Materials, 1999. **1**(4): p. 65-68.

168. Barabasi, A.L. and H.E. Stanley, *Fractal Concepts in Surface Growth*. 1995: Cambridge University Press.

169. Chen, C.-C. and F.C.-N. Hong, *Interfacial studies for improving the adhesion of diamond-like carbon films on steel.* Applied Surface Science, 2005. **243**(1-4): p. 296-303.

170. Xiang, Y., et al., *Investigation on preparation and properties of thick DLC film in medium-frequency dual-magnetron sputtering.* Vacuum, 2005. **80**(4): p. 324-331.

171. Kennedy, F.E., et al., *Tribological behavior of hard carbon coatings on steel substrates.* Wear, 2003. **255**(7-12): p. 854-858.

172. Lung, B.H., M.J. Chiang, and M.H. Hon, *Effect of gradient a-SiCx interlayer on adhesion of DLC films.* Materials Chemistry and Physics, 2001. **72**(2): p. 163-166.

173. Knight, J.C., T.F. Page, and H.W. Chandler, *Thermal instability of the microstructure and surface mechanical properties of hydrogenated amorphous carbon films.* Surface and Coatings Technology, 1991. **49**(1-3): p. 519-529.

174. Lee, S., et al., Thin Solid Films, 1999. **341**: p. 68-.

175. De Martino, C., et al., Diamond & Related Materials, 1997. **6**: p. 559-.

176. Camargo Jr., S.S., et al., Thin Solid Films, 1998. **332**: p. 130-.

177. Bursiková, V., et al., *Temperature dependence of mechanical properties of DLC/Si protective coatings prepared by PECVD.* Materials Science and Engineering, 2002. **A324**: p. 251-254.

178. Bull, S.J. and S.V. Hainsworth, *Time-dependent changes in the mechanical properties of diamond-like carbon films.* Surface and Coatings Technology, 1999. **122**(2-3): p. 225-229.

179. Ozmen, Y., A. Tanaka, and T. Sumiya, *The effect of humidity on the tribological behavior of diamond-like carbon (DLC) film coated on WC-Co by physical vapor deposition method.* Surface and Coatings Technology, 2000. **133-134**: p. 455-459.

180. Ronkainen, H., S. Varjus, and K. Holmberg, *Tribological performance of different DLC coatings in water-lubricated conditions.* Wear, 2001. **249**(3-4): p. 267-271.

181. Persson, K. and R. Gahlin, *Tribological performance of a DLC coating in combination with water-based lubricants.* Tribology International, 2003. **36**(11): p. 851-855.

182. Tallion, T.E., *On competing failure modes in rolling contact.* ASLE Trans., 1967. **10**: p. 418-439.

183. Podgornik, B., et al., *Combination of DLC coatings and EP additives for improved tribological behaviour of boundary lubricated surfaces.* Wear, 2006. **261**(1): p. 32-40.

184. Willermet, P.A., et al., *Mechanism of formation of antiwear films from zinc dialkyldithiophosphates.* Tribology International, 1995. **28**(3): p. 177-187.

185. Martin, J.-M., et al., *Transfer films and friction under boundary lubrication.* Wear, 2000. **245**(1-2): p. 107-115.

186. De Barros, M.I., et al., *Friction reduction by metal sulfides in boundary lubrication studied by XPS and XANES analyses.* Wear, 2003. **254**(9): p. 863-870.

187. Kalin, M., et al., *The lubrication of DLC coatings with mineral and biodegradable oils having different polar and saturation characteristics.* Surface and Coatings Technology, 2006. **200**(14-15): p. 4515-4522.

188. Podgornik, B. and J. Vizintin, *Tribological reactions between oil additives and DLC coatings for automotive applications.* Surface and Coatings Technology, 2005. **200**(5-6): p. 1982-1989.

189. Schaefer, L., et al. *Tribological applications of amorphous carbon and crystalline diamond coatings*. in *43rd Annual Tehcnical Conference of the Society of Vacuum Coaters*. 2000. Denver: Soceity of Vacuum Coaters.

190. Gåhlin, M., M. Larsson, and P. Hedenqvist, *ME-C:H coatings in motor vehicles.* Wear, 2001. **249**: p. 302-209.

191. Brand, J., et al., *Reduzierung von Reibungsverlusten im Ventiltrieb durch Besichtungen.* VDI Berichte, 1999. **1472**: p. 299-312.

192. Arps, J.H., R.A. Page, and G. Dearnely, *Reduction of wear in critical engine components using ion-beam-assisted deposition and ion implantation.* Surface and Coatings Technology, 1996. **84**: p. 579-583.

193. Klingenberg, M., et al., *Practical applications of ion beam and plasma processing for improving corrosion and wear protection.* Surface and Coatings Technology, 2002. **158-59**: p. 164-169.

194. Podgornik, B., S. Jacobson, and S. Hogmark, *DLC coating of boundary lubricated components: advantages of coating one of the contact surfaces rather than both or none.* Tribology International, 2003. **36**: p. 843-849.

195. Tiainen, V.-M., *Amorphous carbon as a bio-mechanical coating -- mechanical properties and biological applications.* Diamond and Related Materials, 2001. **10**(2): p. 153-160.